CHAPTER 3

NEUTRON INDUCED REACTIONS

I. General Principles

If a moving particle collides with another one, kinetic energy is exchanged between them in agreement with the laws of conservation of energy and of momentum. If the potential energy of the system remains unaltered, the kinetic energy being conserved during the collision, the phenomenon is called elastic scattering.

The scattering is inelastic if one of the particles is left in an excited state after the collision. During an inelastic collision with a bombarding particle, an atomic nucleus can present several phenomena:

The nucleus is merely excited to a higher energy level, from which it returns to the ground state by emission of one or more photons. Example: during inelastic collision of Au with ca. 1 MeV neutrons, 260 keV γ-radiation is emitted.

The incident particle is captured and a "compound nucleus" is formed, which is either stable or radioactive. The mass of this compound nucleus is, however, smaller than the sum of the masses of the original nucleus and of the incident particle. Hence photons (prompt gammas) are emitted with an energy, determined by this mass difference, by the kinetic energy of the incident particle and the excitation levels of the compound nucleus. This phenomenon is usually called radiative capture, represented by the (n, γ) symbol, i.e. the (n, γ) reaction.

The incident particle is captured and another elementary particle is emitted, e.g. a proton, α-particle, neutron, etc. i.e. (n, p), (n, α), (n, n'), (n, 2n), . . . reactions.

At very high energies, spallation, fragmentation and fission of the compound nucleus is possible.

It must be borne in mind, that there is a difference between non-elastic and inelastic scattering. Non-elastic scattering is by definition the total cross section minus the elastic scattering, i.e. the inelastic scattering plus all other reactions. In many cases it is the same as the

cross section for inelastic scattering (e.g. bismuth in the MeV region), but should be carefully distinguished from the latter, because of the experimental methods involved and the possibility that in some cases they may be markedly different.

Within the scope of this book neither the fragmentation, spallation and fission reactions nor the elastic collisions are of interest. The most important are those where nucleons are only reorganized. Those reactions are of the general type $A + a \rightarrow B + b$ or abbreviated $A(a, b)B$. The formalism of nuclear reactions is similar to chemical reactions. One can state: the original nucleus A reacts with projectile a, forming product nucleus B, whilst a particle and/or photon b is emitted, liberating or absorbing an energy Q. Hence: $A(a, b)B + Q$. If $Q > 0$, the reaction is exoergic; for $Q < 0$ the reaction is endoergic. As for chemical reactions, one can speak of an "activation energy". Indeed, even for exoergic reactions a certain energy is often needed in the form of kinetic energy of the projectile; this is the case for particles with a positive charge: p, d, t and α-particles and heavier positive ions, because of the Coulomb barrier around the nucleus:

$$E_b = \frac{Z_A Z_a e^2}{R_s} \tag{3.1a}$$

where Z_A, Z_a = number of protons of A, and a respectively,

e = electron charge = 4.8×10^{-10} e.s.u.;

$R_s = R_A + R_a$

If R_A and R_a are expressed in Fermi units (10^{-13} cm), then

$$E_b = 1.44 \frac{Z_A Z_a}{R_s} \quad \text{(MeV)} \tag{3.1b}$$

The nuclear radius may be estimated from eq. (3.30).

For a neutron ($Z_a = 0$), where $E_b = 0$, no activation energy is needed. Hence, the capture of slow or thermal neutrons is usually a favorable process, also because the average binding energy per neutron amounts to ca. 8 MeV.

Note: The Coulomb barrier represents the repulsion between two like-charged particles. It affects not only charged particles coming into the nucleus, but also charged particles leaving the nucleus (see section IIIB of this chapter).

The comparison with chemical reactions also holds for the "com-

pound nucleus" (see further), which can be compared with the "activated complex" in chemical kinetics.

An important difference between chemical and nuclear reactions is due to the fact that the Q-values are not of the same order of magnitude nl. in the MeV range for nuclear reactions and in the eV range for molecular reactions.

II. Properties of Nuclear Reactions—Laws of Conservation

There is no change in total charge: $\sum Z$ = constant.

There is conservation of total energy (E) and of total momentum (mv).

As already stated, chemical binding energy and corresponding forces can be neglected in this connection, except in some reactions with very slow neutrons. Conservation of energy does, however, include the energy, corresponding to the change of mass during the reaction; this is, indeed, the most important fraction of the available kinetic energy. If the total mass diminishes, the corresponding energy ($E = mc^2$) is thus released as kinetic energy of the emitted particles, or as energy of the emitted photons, and of the residual nucleus B. The mass difference in atomic mass units (a.m.u., ^{12}C scale), multiplied with 931, gives this energy in MeV. Tables with isotopic masses can be found in Ref. 1.

III. The Q-Value – Threshold Reactions

(A) Definition of the Q-Value

The Q-value is defined as

$$Q = c^2\left(\sum_{\text{initial}} m_i - \sum_{\text{product}} m_p\right) \tag{3.2}$$

or

$$Q(\text{MeV}) = 931\left(\sum_i m_i - \sum_p m_p\right) \tag{3.3}$$

where m is in a.m.u.

Considering the mass balance, the reaction is called exoergic if $\sum_p m_p < \sum_i m_i$, i.e. $Q > 0$. As no activation energy is needed for neutrons, the reaction will take place with thermal neutrons.

Example: $^{27}Al(n, \gamma)\,^{28}Al + Q$

$\sum_i m_i = 26.981535 + 1.0086654 = 27.990200$ a.m.u.

$\sum_p m_p = 27.981908 + 0 = 27.981908$ a.m.u.

$\sum_i m_i - \sum_p m_p = 0.008292$ a.m.u., $Q = 931 \times 0.008292 = +7.7$ MeV

(7.7 MeV is the excitation energy of the compound nucleus; this energy is liberated as γ-energy). The remaining ^{28}Al nucleus is radioactive.

(B) Definition of Threshold Energy and Effective Threshold Energy

If $\sum_p m_p > \sum_i m_i$, the reaction is endoergic ($Q < 0$). Hence, the incident neutrons must have sufficient kinetic energy, so that the reaction can take place (fast neutrons).

For these reactions there is a so-called threshold, i.e. the minimum energy at which the reaction is possible (E_T). E_T is not only a function of the calculated Q-value (<0), because part of the kinetic energy of the incident particle is only used for the recoil of the compound nucleus as such, without contributing to the increase of the total mass. E_T is somewhat higher than $-Q$, namely:

$$E_T\,(\text{MeV}) \simeq -Q\,(\text{MeV})\,\frac{m_a + m_A}{m_A} \tag{3.4}$$

where, for neutron irradiation, $m_a \simeq 1$.

Example 1: $^{12}C(n, 2n)^{11}C + Q$, or $^{12}C \rightarrow {}^{11}C + n + Q$

$\sum_i m_i = 12.000000$ a.m.u.

$\sum_p m_p = 11.011433 + 1.0086654 = 12.020098$ a.m.u.

$\sum_i m_i - \sum_p m_p = -0.020098$ a.m.u., $Q = -931 \times 0.020098 = -18.71$ MeV

$E_T = 18.71 \times 13.0086654/12.000000 = 20.3$ MeV.

If a nucleus is bombarded with neutrons of energy E_T, this will just be sufficient for the mass increase of that particular endoergic reaction, the emitted particle having theoretically zero kinetic energy. In the case of (n, p) and (n, α) reactions this particle has, however, a positive charge and must have, according to the classical theory,

sufficient energy to overcome the barrier before a reaction can proceed. In the quantum-mechanical treatment of the same problem, there exists a finite probability for reactions to occur with particles having less energy than in the Coulomb barrier treatment, by a mechanism called "tunnelling" (see chapter 6, section IA1). In practice, however, this probability drops rapidly as the energy of the particle decreases below the barrier restriction. The Coulomb barrier for a given reaction can be calculated by means of eq. (3.1b) and (3.30) and will be at an energy higher than E_T. It is obvious that Z_A and R_A are the charge and radius respectively of the product nucleus.

Example 2: $^{52}_{24}\mathrm{Cr(n, p)}\,^{52}_{23}\mathrm{V}$

$$\sum_i m_i - \sum_p m_p = 52.9491794 - 52.9526252 = -0.0034458 \text{ a.m.u.}$$

$$Q = -0.0034458 \times 931 \text{ MeV} = -3.21 \text{ MeV}$$

$$E_T = 3.21 \times 52.9491794/51.940514 = 3.27 \text{ MeV}$$

$$E_b = \frac{1.44 \times 23 \times 1}{1.5 \times 52^{1/3} + 1.5 \times 1^{1/3}} \simeq 4.7 \text{ MeV}$$

Example 3: $^{55}_{25}\mathrm{Mn}\ (\mathrm{n}, \alpha)\ ^{52}_{23}\mathrm{V}$

$$\sum_i m_i - \sum_p m_p = 55.9467104 - 55.947404 = 0.000685 \text{ a.m.u.}$$

$$Q = -0.64 \text{ MeV and } E_T \simeq 0.65 \text{ MeV}$$

$$E_b = \frac{1.44 \times 23 \times 2}{1.5 \times 52^{1/3} + 1.5 \times 4^{1/3}} \simeq 8.3 \text{ MeV}.$$

This is important for activation analysis. Although E_T for the reaction $^{55}\mathrm{Mn(n, \alpha)}$ is lower than that for the reaction $^{52}\mathrm{Cr(n, p)}$, its Coulomb barrier is considerably higher. Hence it is possible to determine chromium via $^{52}\mathrm{V}$ without interference from manganese, when using 7 MeV neutrons, for instance (variable-energy cyclotron, see chapter 7, section IVB).

Obviously, the penetrability of the charged particle increases with $E - E_T$ (see Figure 3.1). In the case of reactor neutrons, which are not monoenergetic, their energy distribution $f(E)$ must be considered (fission spectrum); $f(E)$ is the fast neutron flux density per unit energy interval (see this chapter, section V, C3b). If the probability for the nuclear reaction is represented by $\sigma(E)$ ("cross section", see section V of this chapter), the reaction rate as a function of energy will be given by $f(E)\sigma(E)$. This product, the so-called "response function", is also plotted in Figure 3.1. The total reaction rate is $\int_0^\infty \sigma(E)f(E)\,\mathrm{d}E$, i.e. area ABC. In fact it is this response integral which results directly from the measurement of the induced activity. Note that $\sigma(E)$ is proportional to the penetrability $P(E)$ (*cf.* eq. (6.1)).

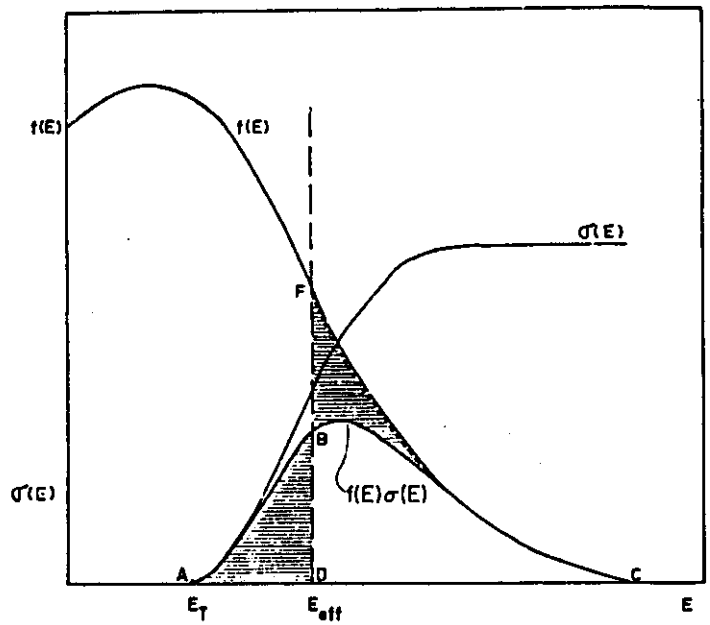

Fig. 3.1. Definition of effective threshold (2). (Permission of Hughes, D. J., *Pile Neutron Research*, 1953, Adison-Wesley, Reading, Mass.)

According to Hughes (ref. 2, p. 96) an effective threshold E_{eff} can be defined so that area ABC is equal to area DFC, or area ABD equal to area BFC, and that the observed reaction rate is in fact the same, as if all the neutrons above E_{eff} are equally effective in producing the reaction, but none below this energy.

In other words: the value E_{eff} is chosen in such a way, that the $\sigma(E)$ or probability curve is approximated by a step function $\sigma(E) = 0$ for $E < E_{\mathrm{eff}}$; $\sigma(E) = \sigma_{\mathrm{eff}}$ for $E \geq E_{\mathrm{eff}}$ and that the condition

$$\int_{E_T}^{\infty} \sigma(E)f(E)\,\mathrm{d}E = \sigma_{\mathrm{eff}} \int_{E_{\mathrm{eff}}}^{\infty} f(E)\,\mathrm{d}E \qquad (3.5)$$

is fulfilled; σ_{eff} is the reaction cross section for a penetrability = 1, i.e. the maximum value of the $\sigma(E)$ curve. In most cases σ_{eff} can approximately be replaced by the cross section for 14 MeV neutrons. In nearly all cases the $f(E)$ distribution used in this method for determining E_{eff} is taken equal to the fission neutron spectrum (see equation 3.37). The best method for determining the effective threshold energy of a reaction is to derive it from the experimental excitation function, (instead of the theoretical $\sigma(E)$ or $P(E)$ function, see eq. (6.1)) using the definition of E_{eff} and σ_{eff} as given by Grundl and Usner (3) and performing the calculations with a computer. There is also a semi-empirical approach, described by Jung (4). In this book, reference will always be made to Figure 3.1, taken from Hughes (2).

Note that E_{eff} has no exact physical meaning, since it depends on the form of neutron spectrum, which can be slightly different for different reactors and/or irradiation positions.

The difference $E_{eff} - E_T$ is obviously a function of the charge of the nucleus and of the emitted particle, as appears from Figure 3.11. The estimated effective thresholds in a fission spectrum for the above examples 2 and 3 are thus $E_{eff} \simeq E_T + 4 \simeq 7.2$ MeV and $E_{eff} \simeq E_T + 8 \simeq 8.6$ MeV respectively. For the reaction $^{27}Al(n, \alpha)^{24}Na$, having an $E_T = 3.3$ MeV, one finds $E_{eff} \simeq 3.3 + 5.2 \simeq 8.5$ MeV.

Some reactions are called threshold reactions, although $Q > 0$. In this case $E_T < 0$ (equation 3.4), but E_b and $E_{eff} > 0$.

Examples:

	E_T(MeV)	E_{eff}(MeV)
$^{58}Ni(n, p)^{58}Co$	−0.64	2.6–4.1
$^{35}Cl(n, p)^{35}S$	−0.62	2.5
$^{64}Zn(n, p)^{64}Cu$	−0.21	4.0–4.8
$^{54}Fe(n, \alpha)^{51}Cr$	−0.87	9.1

Practically one can say that, after collision of such a nucleus with a thermal neutron, the reaction is possible; however, the "produced" p or α-particle cannot emerge from the compound nucleus and no reaction occurs. Actually a (n, p) or (n, α) reaction will take place with fast neutrons only.

Obviously, for calculating the threshold energy in this case, equation (3.4) must be replaced by

$$E_T(\text{MeV}) = -Q(\text{MeV}) \qquad (3.6)$$

This value takes into account the potential barrier energy of the particular nuclide and the energy distribution of the neutrons in the reactor.

(C) OTHER CONSIDERATIONS IN CONNECTION WITH THE Q-VALUE

Considering the mass and kinetic energy of the nuclei and particles involved in the nuclear reaction, and starting from the law of conservation of energy, it can be proved (see e.g. ref. 5) that

$$Q = E_b\left(1 + \frac{m_b}{m_B}\right) - E_a\left(1 - \frac{m_a}{m_B}\right) - \frac{2\sqrt{(m_a E_a m_b E_b)}}{m_B}\cos\theta \qquad (3.7)$$

on condition that A is initially at rest and that the energies are not too high; θ is the angle between the incident (directed) beam of a and the emission direction of b. This classical expression thus relates strictly the energy E_b and the emission angle θ, assuming a directed beam a.

Example: The exoergic reaction T(d, n)^{4}He with a beam of 100 keV deuterons produces neutrons, whose energy varies from 14.64 MeV in the direction of the beam ($\theta = 0°$) to 13.49 MeV in the opposite direction ($\theta = 180°$). Average value: 14.06 MeV.

T(d, n)^{4}He: $\sum_i m_i = 3.0160494 + 2.0141022 = 5.0301516$ a.m.u.

$\sum_p m_p = 1.0086654 + 4.0026036 = 5.0112690$ a.m.u.

$\sum_i m_i - \sum_p m_p = 0.0188826$ a.m.u., $Q = +17.58$ MeV

without taking into account the contribution of the deuteron (kinetic energy of 0.1 MeV). The released energy is distributed between the reaction products, inversely proportional with their masses, nl. 4.0026036 a.m.u. (^{4}He) and 1.0086654 a.m.u. (^{1}n) (total mass 5.0112690 a.m.u.).

Thus ^{4}He: $17.57 \times 1.0086654/5.0112690 = 3.54$ MeV

^{1}n: $17.57 \times 4.0026036/5.0112690 = 14.04$ MeV (E_b).

The value of E_b can also be calculated from eq. 3.7, setting $\theta = 90°$, $\cos\theta = 0$. One finds 14.07 MeV.

The distribution of the neutron energy as a function of angle is given in Table 3.1, taking into account the kinetic energy of the bombarding neutrons. This is of interest for the study of the neutron generator.

TABLE 3.1

Neutron energy from the T(d, n)^{4}He reaction as a function of angle (after Prud'homme (6))

θ (degrees)	Neutron Energy (MeV)	
	100 keV deuterons	150 keV deuterons
0	14.64	14.74
45	14.46	14.54
90	14.06	14.06
135	13.65	13.61
180	13.49	13.42

It is obvious that several Q-values can exist for the same target nucleus and the same bombarding particle, if more than one reaction is possible.

Example:

$^{27}Al(n, \gamma)^{28}Al + Q_1$; $Q_1 = 7.7$ MeV

$^{27}Al(n, p)^{27}Mg + Q_2$; $Q_2 = -1.83$ MeV; $E_T = 1.9$ MeV; $E_{eff} = 4.4$–5.4 MeV

$^{27}Al(n, \alpha)^{24}Na + Q_3$; $Q_3 = -3.14$ MeV; $E_T = 3.3$ MeV; $E_{eff} = 7.3$–8.8 MeV

Bombardment with 1 MeV neutrons will only produce the (n, γ) reaction (and particularly scattering, this phenomenom having an even greater probability for light elements, see further). With increasing neutron energy, the probability for (n, p) and even (n, α) reactions will also increase (*cf.* Figure 3.1, Figure 3.16 and Figure 3.17).

IV. Models of Nuclei – Compound Nucleus – Excited States in Nuclear Reactions

(A) Models of Nuclei

It is interesting to consider here the behavior of the nucleus during the nuclear reaction. Like an atom, that includes a system of electrons, the nucleus (particularly a light nucleus) can be considered as a system

of nucleons and described by a "shell model" with quantum numbers. The behavior of the nucleons in the nucleus is, however, so complex and their interaction so strong that it becomes difficult to study details of the nuclear structure and statistical methods, treating the nucleus as a whole, are a better approximation of the problem. The "uniform model" (Wigner), the "liquid drop model" (Bohr, Wheeler, Frenkel) and the "collective model" (Bohr, Mattelson) start from that point of view.

The "liquid drop model" has found much application in the explanation of nuclear reactions and is of interest within the scope of this book. In this model, the nucleus is compared to an incompressible liquid drop. The nucleons are moving in the nucleus with a certain kinetic energy, comparable to the thermal movement of molecules in a liquid drop. Increasing temperature causes evaporation of those molecules; similarly, the nucleons are said to evaporate if the nucleus is sufficiently excited.

(B) Nuclear Reactions–Compound Nucleus

If some particle interacts with the electron cloud of an atom, it collides with only one particular electron. In the case of the shell model, the same picture should be expected for reactions in the nucleus. However, owing to the "dense" structure of the nucleus, the processes are different. The mutual interaction of the nucleons is so strong, that the impact energy of the incident particle is very rapidly distributed over the whole nucleus. The nucleus remains in an excited state, during a certain finite time (about 10^{-14}–10^{-15} s), which is long compared to the time required to traverse the nucleus: if $E_n = 100$ eV, $v_n = 10^7$ cm s^{-1} and $t = 10^{-12}$ cm/10^7 cm s^{-1} = 10^{-19} s. Hence one can state that the nucleus has captured the neutron and that there exists a "compound nucleus" (Bohr, 1935) comparable to the "activated complex" in chemical kinetics; ex. $^{27}Al + n \rightarrow {}^{28}Al^*$.

The compound nucleus is highly excited (symbol *) due to the high binding energy of the neutron, plus possibly its kinetic energy. De-excitation is possible in several ways, e.g. by emission of a particle (p, α, n, 2n, d . . .) or of electromagnetic radiation (γ). Each of these processes has a certain probability, independent of the way of formation of the compound nucleus (due to the rapid distribution of the incident energy over all the nucleons) but only dependent on its excitation level.

Several deexcitation processes are sometimes probable, e.g.

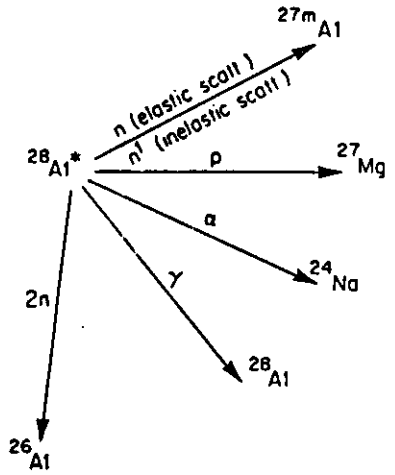

Generally: $A + a \rightarrow C^*$; $C^* \rightarrow B_1 + b_1 + Q_1$, or $C^* \rightarrow B_2 + b_2 + Q_2$, etc.

The probability for one of these reactions after neutron capture is given by the corresponding "cross section": σ(n, p), σ(n, α), σ(n, γ), σ(n, 2n). Their values at 5 MeV neutron energy are:

σ(n, p) = 0.03 barn

σ(n, α) = 0.001 barn

σ(n, γ) = 5.10^{-5} barn

σ(n, n) + σ(n, n') = 0.8 barn

σ(n, 2n) = ...

σ(n, x) is the probability of capture of a neutron multiplied by the relative probability of emission of x (see further).

The notion "cross section" and the corresponding unit (barn) are given in section V A. The influence of the neutron energy on σ is treated in this chapter, section V C.

(C) Excited States

Considering the excitation levels of the compound nucleus, one can distinguish bound states, whose energies are smaller than the binding

energy of the weakest bound nucleon, and from which deexcitation occurs by gamma emission and virtual states, from which deexcitation by emission of gamma rays or nucleons is possible. With increasing excitation energy the level density increases (see Figure 3.2).

Experimental evidence for these excitation levels is found during the capture of nucleons. The compound nucleus C formed has an excitation energy corresponding to the mass difference $A + a - C$ (= binding energy of nucleon a, e.g. 7.7 MeV for a neutron in ^{28}Al), plus the kinetic energy of the captured nucleon.

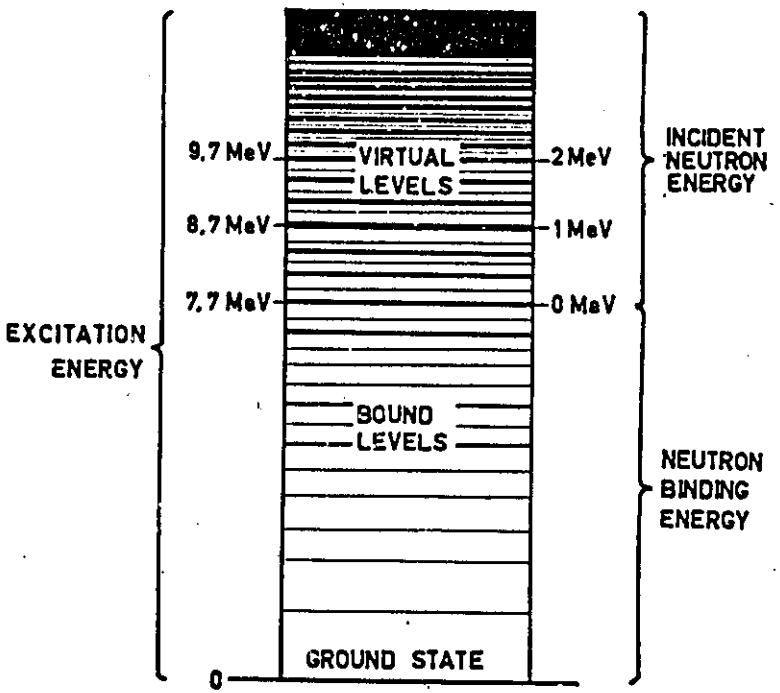

Fig. 3.2. Energy levels of compound nucleus, formed by neutron capture in ^{27}Al with a binding energy of 7.7 MeV (2). (Permission of Hughes, D. J., *Pile Neutron Research*, 1953, Adison-Wesley, Reading, Mass.)

This total amount can exactly coincide with an existing energy level of the compound nucleus. In that case the reaction will occur with a high yield (resonance) (Figure 3.4). From the resonance energy, the nuclear energy levels can be calculated.

Example: During the neutron irradiation of ^{103}Rh, a ^{104}Rh compound nucleus is formed, with a resonance at $E_n = 1.260$ eV. The binding energy of a neutron in Rh* is 6.8 MeV (see Ref. 7), hence one can state that 6.8 MeV + 1.260 eV is a virtual state of the ^{104}Rh compound nucleus (*cf.* Figure 3.2). Deexcitation from this level by γ-emission occurs very rapidly after the neutron capture ($\sim 4.10^{-15}$s), forming ^{104m}Rh($T_{1/2} = 4.3$ m) and ^{104}Rh ($T_{1/2} = 44$ s), which are radioactive (respectively I.T., β^- and β^-, γ).

These nuclear energy levels are not infinitely sharp, but have a finite width, in agreement with the uncertainty principle of Heisenberg:

$$\Gamma\tau = \frac{h}{2\pi} = \hbar = 0.65 \times 10^{-15}\ \text{eV s} \tag{3.6}$$

where: τ = average life of the nucleus in a given energy level;
Γ = level width.

i.e. if $\tau = 10^{-15}$ s, the level width is 0.65 eV. Or, if $\Gamma = 0.156$ eV, as is the case for ^{104}Rh, the average life of the nucleus in that energy level (6.8 MeV + 1.260 eV) is about 4.10^{-15} s.

If in a given state, τ is very short ($\Gamma/\hbar$ large), decay from that state is very probable: $\Gamma/\hbar$ is a measure for the disintegration probability per second from a given energy state.

A level with $\Gamma = 10^4$ eV = 10 keV ($\tau = 6.5 \times 10^{-19}$ s) is considered as a typical "wide level". This case occurs frequently with light nuclei (*cf.* Figure 3.4). If $\Gamma = 0.1$ eV = 100 mV ($\tau = 6.5 \times 10^{-14}$ s) the level is considered as "typically sharp".

As already stated, deexcitation from a certain energy level is possible in several ways: emission of a particle (p, α, n ...) or a photon. The probabilities for each of these processes can be expressed as "partial level widths", Γ_p, Γ_α, Γ_n, Γ_γ ...

$$\Gamma = \Gamma_\gamma + \Gamma_n + \Gamma_p + \Gamma_\alpha + \dots \tag{3.7}$$

The relative probability for emission of γ, n, p ... is then given by

$$\Gamma_\gamma/\Gamma,\ \Gamma_n/\Gamma,\ \Gamma_p/\Gamma \dots \tag{3.8}$$

The overall probability $\sigma(n, x)$ for the reaction (n, x) is given by

$$\sigma(n, x) = \sigma_C \times \Gamma_x/\Gamma \tag{3.9}$$

where σ_C = probability for the formation of a compound nucleus
Γ_x/Γ is defined in equation (3.8).

The physical meaning of σ will be discussed under section V A of this chapter.

Remark: If the nucleus is very highly excited (>15 MeV) several nucleons can be emitted at the same time. As 1 eV corresponds to about 11,000°C, such a nucleus is said to have a very high nuclear temperature and the corresponding emission phenonemon is called "evaporation".

V. Cross Sections in Neutron Induced Reactions

(A) Definition

If a target with N nuclei per cm^3, each of them having an effective area

$$\sigma = \pi R_A^2 \text{ (in cm}^2\text{)} \tag{3.10}$$

is placed in a neutron beam (flux φ neutrons cm^{-2}s^{-1}), the number of collisions will be given by

$$\text{collisions per cm}^3 \text{ per s} = \varphi\sigma N \ (\text{cm}^{-3}\,\text{s}^{-1}) \tag{3.11}$$

The assumption is made that "overlapping" of the nuclear areas is negligible, i.e. the target must be a very thin foil.

The number of collisions can also be considered as proportional to the flux and to the number of target nuclei per cm^3, the proportionality constant being the cross section of the nucleus.

This simple consideration leads to the definition of the collision cross section

$$\sigma_{col}\ (\text{cm}^2) = \frac{\text{collisions (cm}^{-3}\text{s}^{-1})}{\varphi(\text{cm}^{-2}\text{s}^{-1})N(\text{cm}^{-3})} \tag{3.12}$$

The cross section is expressed in units of area (cm^2), or better in barns, abbreviation b(1b = 10^{-24} cm^2). Indeed, the radius of a nucleus is given approximately by eq. (3.30), so that, for $A = 125$, $R \simeq 7.5 \times 10^{-13}$ cm; hence $\sigma = \pi R^2 \simeq 1.5 \times 10^{-24}$ cm^2. Hence σ appears to be of the order of a few barns and this is why the unit is so chosen. Parts of the barn are: mb = 10^{-3}b and μb = 10^{-6}b.

If the neutrons are multidirectional – as is the case in a reactor – the neutron flux is more conveniently defined as the product of the neutron density times the neutron velocity. Within the scope of this book,

the "conventional" neutron flux φ (neutrons $cm^{-2}s^{-1}$) will be identified with n(neutrons cm^{-3}) $\times$ v(cm s^{-1}).

In the above discussion, the actual phenomena during and particularly after the collision have not been considered. There are several possibilities: neutron scattering, elastic (n, n) or inelastic (n, n'); emission of photons or particles: (n, γ), (n, p), (n, α), ... If the partial level width for such a process is given by Γ_γ, Γ_p, Γ_α, Γ_n ..., the relative probability for the emission of x ($x = \gamma$, n, p, α ...) is Γ_x/Γ, where $\Gamma = \Gamma_\gamma + \Gamma_p + \Gamma_\alpha + \Gamma_n$ (see IV B and C).

One particular possibility of the nuclear reaction is then represented by the corresponding reaction cross section $\sigma(n, x)$:

$$\sigma(n, x) = \sigma_C \Gamma_x/\Gamma \tag{3.9}$$

as already stated above. Here, σ_C is the probability for the formation of a compound nucleus.

(B) Practical Considerations

The various conventions and definitions of thermal, resonance and fast fluxes and cross sections are discussed by Stoughton and Halperin (8), Westcott (9,10), Zijp (11,12) and Høgdahl (14). Normally one distinguishes the following cross sections (Hughes 2 and 13).

1. *Thermal neutron cross sections*

Thermal neutrons are neutrons having the most probable velocity v_0 of the Maxwellian distribution at 20°C, nl. 2200 m/s, or an energy of 0.025 eV.

(a) Reaction cross sections. Refer to all cases in which the neutron is not reemitted, i.e. to (n, γ), (n, p), (n, α) and (n, f) reactions. Practically all the reaction cross sections for $Z < 88$ are for (n, γ)'s, unless explicitly stated. As will be shown later, the reaction rate in a thermal flux can be calculated from the knowledge of the cross section (σ_0) at the particular velocity v_0, on condition that $\sigma(v) \propto 1/v$. Other authors define the reaction cross section as the sum of the cross sections of all interactions, excepting elastic scattering.

The absorption cross sections, σ_{abs} are those particular reaction cross sections that are measured by observing the reaction itself in which the neutron is absorbed. The principal methods used for their

determination are described by Hughes (2): the pile oscillator, the difference $\sigma_T - \bar{\sigma}_s$, some extrapolation methods. For activation analysis purposes, the absorption cross section is of great importance to calculate neutron shielding effects (see chapter 10).

The activation cross sections σ_{act}, for thermal neutrons mainly $\sigma(n, \gamma)$, sometimes $\sigma(n, p)$, $\sigma(n, \alpha)$, $\sigma(n, f)$, are most commonly determined from the radioactivity of the product nucleus. This determination implies the production of a radioactive isotope. Naturally, σ_{act} refers to one particular isotope, hence it is an isotopic cross section; for monoisotopic elements it is the atomic cross section as well. For activation analysis, the value of σ_{act} allows the calculation of the induced activity by a given nuclear reaction.

(b) Scattering cross sections. Are usually constant with energy in the thermal region. They are particularly important for light nuclei and/or at higher neutron energies.

Physically one distinguishes several kinds of scattering, with corresponding cross sections: coherent scattering cross section (σ_{coh}), free atom cross section (σ_{fa}), average scattering cross section ($\bar{\sigma}_s$), differential scattering cross section $d\sigma/d\Omega$ for scattering at a given solid angle (φ, θ).

Within the scope of this book, only $\bar{\sigma}_s$ is of interest.

(c) Total cross section σ_T. Is determined by transmission measurements and is considered to be accurate, as the intensity of the neutron beam is measured without and with the sample respectively (Figure 3.3). The presence of the sample in the beam causes the disappearance of a certain neutron fraction either by scattering or by absorption. In many cases radioactive nuclides are formed by absorption.

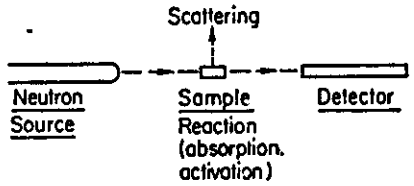

Fig. 3.3. Apparatus used for measuring total neutron cross section.

Obviously, the total neutron cross section includes the scattering as well as the reaction cross section:

$$\sigma_T = \sigma_{abs} + \bar{\sigma}_s \tag{3.13}$$

as is apparent in the following examples:

Element		$\sigma_T(b)$	$\sigma_{abs}(b)$	$\bar{\sigma}_i(b)$
Co	100% ^{59}Co	44	37.0	7
Sc	100% ^{45}Sc	50	24.0	24
Mn	100% ^{55}Mn	15.5	13.2	2.3
Sb	57.25% ^{121}Sb; 42.75% ^{123}Sb	10	5.7	4.3
Cu	69.1% ^{63}Cu; 30.9% ^{65}Cu	11	3.77	7.0

If the reaction leads to only one radioactive isotope, then $\sigma_{act} = \sigma_{abs}$ in the case of a monoisotopic element.

Example:

Element		σ_{abs} (b)	σ_{act} (b)
Mn	100% ^{55}Mn	13.2 ± 0.4	13.4 ± 0.3
Sc	100% ^{45}Sc	24.0 ± 1.0	10 ± 4 (20 s) 12 ± 6 (85 d) 20 s + 85 d (20 s → 85 d): 22 ± 2

In the case of polyisotopic elements, the same reasoning holds.

Example: the absorption and activation cross sections of the natural isotopes of copper, ^{63}Cu and ^{65}Cu, were determined separately:

Element		σ_{abs} (b)	σ_{act} (b)
Cu	^{63}Cu (69.1%)	4.3 ± 0.3	3.9 ± 0.8 (12.8 h)
	^{65}Cu (30.9%)	2.11 ± 0.17	1.3 ± 0.4 (5.14 m)
		determined after separation of isotopes	

If the values of σ_{abs} are not determined for each of the natural isotopes, one can state $\sigma_{abs} = \bar{\sigma}_{act}$ (average) $= \sigma_{1act}\theta_1 + \sigma_{2act}\theta_2 \ldots$, where θ = isotopic abundance.

Example:

Element	σ_{abs} (b)	σ_{act} (b)
Ir ^{191}Ir (38.5%) ^{193}Ir(61.5%)	430 ± 20 (for element)	260 ± 100 (1.4 m) 700 ± 200 (74 d) 130 ± 30 (19 h) 960 (1.4 m → 74 d) $\bar{\sigma}_{act}$ = (0.385 × 960) + (0.615 × 130) = 450

If by neutron capture stable isotopes are formed, it is obvious that $\bar{\sigma}_{act} < \sigma_{abs}$.

Example:

Isotopes	% abundance	σ_{abs}	σ_{act}
Cd–element	—	2,450 ± 100 b	
^{106}Cd	1.22		1.0 ± 0.5 b (6.7 h)
^{108}Cd	0.87		
^{110}Cd	12.39		0.2 ± 0.1 b (49 m)
^{111}Cd	12.75		
^{112}Cd	24.07		30 ± 15 mb (14 y)
^{113}Cd	12.26	20,000 ± 300 b	
^{114}Cd	28.86		0.14 ± 0.03 b (43 d) 1.1 ± 0.3 b (2.3 d)
^{116}Cd	7.58		1.5 ± 0.3 b (2.9 h)

The neutron absorption is almost completely due to ^{113}Cd (indeed, 20,000 b × 0.1226 = 2,450 b), forming nonactive ^{114}Cd by (n, γ) reaction. Hence $\bar{\sigma}_{act} < \sigma_{abs}$ for this element.

(d) Macroscopic cross section Σ. All the cross sections defined above are called microscopic cross sections, as they refer to a particular nucleus. For some purposes, a macroscopic cross section (Σ_{abs}; $\bar{\Sigma}_i$) is used, defined by

$$\Sigma = \sigma N = \sigma \frac{\delta N_A}{A} \tag{3.14}$$

thus taking directly the density δ(g cm^{-3}) and the atomic weight A

of the sample into account; N_A = Avogadro's number and N = number of atoms per cm³. Note that the dimension of Σ is cm^{-1}, whereas σ is in cm^2.

The macroscopic absorption or scattering cross section can also be calculated if several types of nuclei are present: Σ = sum of $\sigma_i N_i$.

2. *Resonance parameters*

The literature gives also tables with resonance parameters and neutron cross section curves (e.g. ref. 13). Indeed, σ is energy dependent and resonances can occur at certain energies. The data normally include: the resonance energy $E_o(E_r, T_r)$, the total level width Γ and the partial level widths Γ_α, Γ_p, Γ_γ, Γ_n, Γ_f in keV, eV or mV (=10^{-3} eV).

Remark: the tabulated values do not always correspond with the drawn cross section curves, as some corrections are made, such as Doppler broadening (because the assumption that the nucleus is in rest is not always justified), self absorption, etc.

For heavy nuclei the resonance is mostly due to a (n, γ) reaction, for light nuclei, however, to scattering and sometimes to a (n, α) or a (n, p) reaction, as can be seen from some typical examples, given in Table 3.2.

TABLE 3.2
Examples of resonance parameters

Isotope	Resonance energy	Level widths
$^{180}_{73}$Ta	0.433 ± 0.004 eV	Γ_γ = 30 ± 5 mV, Γ_n = 0.12 ± 0.02 mV
$^{98}_{42}$Mo	45.0 ± 0.4 eV	Γ_γ = 210 ± 60 mV, Γ_n = 174 ± 10 mV
$^{6}_{3}$Li	284 ± 4 keV	Γ = 90 ± 10 keV, Γ_n = 60 ± 15 keV Γ_α = 30 ± 10 keV ($\Gamma = \Gamma_n + \Gamma_\alpha$; $\Gamma_\gamma \approx 0$)

The characteristic resonance parameters of some important nuclides are given in Table 10.3.

In the neighborhood of E_r, the energy dependence of σ(n, γ) and $\bar{\sigma}_g$ is described by the Breit–Wigner formula, which is comparable to the optical dispersion formula. In section V, C2 of this chapter an interesting quantity I, called resonance integral cross section, will be defined.

3. *Neutron cross-section curves, $\sigma(E)$*

These curves represent the cross section as a function of neutron energy. In most cases the total cross section is given (σ_T), although sometimes σ(n, γ), σ(n, p), σ(n, α), σ(n, 2n), σ(n, n') = σ_{inel}, $\sigma_{n.a.}$ (non-elastic) = $\sigma_T - \sigma_{el}$, σ(n, f) ... are explicitly plotted, particularly in recent editions (e.g. ref. 13, 2nd ed.). Normally atomic cross sections are given, i.e. for the natural element (ex.: $_{48}$Cd); if, however, the mass number of a specific isotope is indicated (ex.: $^{135}_{54}$Xe, $^{147}_{67}$Pm), the cross section is obviously the isotopic one.

The resonance peaks, as seen in the figures, do not correspond to the actual ideal form of that resonance, as the accuracy of the measurements depends on the resolution of the apparatus in the energy region concerned. (This resolution is schematically represented in the figures by an equivalent triangle, Δ, δ, ...).

Example: for the 6.7 eV resonance in $_{92}$U, the figure (13) shows $\sigma_r(E_r)$ = 4000 b. With a perfect resolution, this should be 8000 b. Correction for Doppler broadening should finally yield 23,000 b.

The cross section curve of rhodium, showing a typical resonance, is represented in Figure 3.4. The corresponding resonance parameters are E_r = 1.257 ± 0.002 eV, Γ_γ = 155 ± 4 mV, Γ_n = 0.78 ± 0.01 mV $\sigma_r(E_r)$ = 5000 ± 200 b, I_{act} = 650 b (resonance integral, see section V, C2). For thermal neutrons (2200 ms^{-1}):

σ_T = 154 b

$\bar{\sigma}_g$ = 5.5 ± 1.0 b

σ_{abs} = 149 ± 4 b; σ_{act} = $\begin{cases} 12 \pm 2 \text{ b (4.5 m } ^{104m}\text{Rh)} \\ 140 \pm 30 \text{ b (44 s } ^{104}\text{Rh)} \end{cases}$ $\Big\}$ (4.5 m → 44 s) 152 b

(C) Calculation of Reaction Rates for Reactor and Accelerator Irradiations

1. *Thermal and epithermal neutrons in the reactor*

(a) General considerations. Thermal neutrons have a most probable energy of 0.025 eV (velocity v_0 = 2200 m/s) whereas neutrons with an energy of 0.1 – 1 eV are sometimes called epithermal neutrons. In this region σ_T is mostly proportional to $E^{-1/2}$ or to $1/v$ ("1/v-law"), see Figure 3.4. Widely different σ-values are found for different iso-

topes and no general rule can be given. The values for σ_T, σ_{abs} and $\bar{\sigma}_i$ for thermal neutrons are given in Appendix 1, Table 1.

Thermal and epithermal neutrons mainly give (n, γ) reactions – or scattering for light nuclei – unless explicitly stated. As (n, γ) reactions often yield stable isotopes, it is obvious that neutron absorption not always induces radioactivity, i.e. $\sigma_{act} < \sigma_{abs}$, example $^1H(n, \gamma)^2H$ (stable), $\sigma_{abs} = 0.332$ b, $\sigma_{act} \approx 0$.

A table with activation cross sections is given in the Appendix 1, Table 2.

(b) Calculation of thermal activation (1/v-absorber). As already stated above (*cf.* Figure 3.1), the reaction rate can be calculated, if the neutron energy (or velocity) distribution and the activation cross section curve are known, i.e. $dR = \sigma(E) \times \varphi(E)\,dE$ or $\sigma(v)n(v)v\,dv$ integrated over all the neutron energies (or velocities).

The reaction rate per target nucleus in a sample, where neutron attenuation is negligible, can obviously be represented by

$$R = \int_0^\infty n(v)v\sigma(v)\,dv \tag{3.15}$$

where $n(v)\,dv$ is the density of the neutrons having a velocity between v and $v + dv$ and $\sigma(v)$ the activation cross section for a neutron velocity v.

As mostly $\sigma \propto 1/v$, one can write for a pure $1/v$-absorber

$$\sigma(v) = \sigma_0 v_0/v \tag{3.16}$$

Hence

$$R = v_0\sigma_0 \int_0^\infty n(v)\,dv = nv_0\sigma_0 \tag{3.17}$$

where $n = \int_0^\infty n(v)\,dv$ is called the thermal neutron density.

Consequently, equation (3.15), which is difficult to handle, can be replaced by the simple relationship $R = nv_0\sigma_0$, or $R = \varphi_0\sigma_0$, where φ_0 is the "conventional thermal flux".

Thus, the reaction rate in a thermal neutron flux of known density n can be calculated from the knowledge of the cross section σ_0 at a particular velocity v_0, on condition that $\sigma(v) \propto 1/v$. The velocity v_0 is taken as 2.2×10^5 cm s^{-1}, the most probable velocity of a Maxwellian distribution at 20°C (corresponding energy 0.025 eV). If the $\sigma(v)$-curve shows important resonance peaks, equation (3.17) must be replaced by equation (3.27).

The cross sections in Table 2 (Appendix 1) are given for this velocity v_0, except in some cases where they refer to an average reactor neutron spectrum (values with asterisk). The activation cross sections are for (n, γ) reactions, except when explicitly stated (n, p) or (n, α). For heavy nuclides ($Z > 88$) the cross section for fission is also included.

For practical use in activation analysis (induced activity calculations, see equations (5.36), (5.44), (5.52), (5.53), (5.59), or the more practical equation (10.1)), the per cent abundance of the target isotope in the natural element and the half life of the product nucleus are also given in this Table.

(c) Thermal absorption. In most cases it is permissible to use the 2200 m/s cross section (see foregoing paragraph). The case of neutron diffusion is one of the few instances where other values must be used. Indeed, unlike the case of a reaction rate, which does not depend on neutron temperature, the diffusion length or mean free path l of a neutron is determined by the absorption cross section and is obviously a function of the neutron temperature. It can be shown that the cross section to be used is quite specific the average cross section $\sigma(\bar{v})$ ($\bar{v}$ = average velocity of the neutrons in a Maxwell distribution):

$$l = 1/\sum N_i\sigma(\bar{v})_i \tag{3.18}$$

where N_i = number of nuclides i per cm^3;
$\sigma(\bar{v})_i$ = average absorption cross section for ith nuclide, defined by

$$\sigma(\bar{v})_i = \frac{\int_0^{v_1} n(v)v\sigma(v)_i\,dv}{\int_0^{v_1} n(v)v\,dv} \tag{3.19}$$

v_1 corresponds to the cadmium cut-off energy, e.g. 0.55 eV (see VI, A); $n(v)$ is the neutron density distribution per unit velocity interval. If the analytical expression for $n(v)$ is unknown, an approximate value for $\sigma(\bar{v})_i$ can be obtained by assuming $n(v)$ to be a Maxwellian distribution function, and setting $v_1 = \infty$.

$$\sigma(\bar{v})_i = \sigma_{0i}\frac{\sqrt{\pi}}{2}\left(\frac{293.6}{T_m}\right)^{1/2} \tag{3.20}$$

where σ_{0i} = 2200 m/s absorption cross section for ith nuclide (see Table 1, Appendix 1)
T_m = Maxwellian temperature.

A simple way to find equation (3.20) is as follows.

$$R = nv_0\sigma_0 = n\bar{v}\sigma(\bar{v}) \quad \text{or} \quad \sigma\pi(\bar{v}) = R/n\bar{v} = \frac{v_0\sigma_0}{\bar{v}}.$$

In Chapter 4 (equation (4.17)) it will be shown that the average velocity of the Maxwell distribution $\bar{v}$ is larger than the most probable velocity v_0 by a factor

$$\frac{2}{\sqrt{\pi}}\left(\frac{T_m}{T_0}\right)^{1/2},$$

hence

$$\sigma(\bar{v}) = v_0\sigma_0/v_0\frac{2}{\sqrt{\pi}}\left(\frac{T_m}{T_0}\right)^{1/2} = \sigma_0\frac{\sqrt{\pi}}{2}\left(\frac{T_0}{T_m}\right)^{1/2} \text{ where } T_0 = 293.6°\text{K}.$$

This value $\sigma(\bar{v})$ can be used to compute thermal neutron shielding effects, as outlined in Chapter 10, section II, B, 4b (2).

A cumulative bibliography of the literature on (microscopic) neutron cross sections and allied data, called CINDA (Computer Index of Neutron Data) is available. It is intended primarily to indicate where in the journal and report literature information can be found; it is not a listing of the data themselves (Ref. 30).

2. *Intermediate energy – Resonance neutrons in the reactor*

(a) General considerations. σ_T changes rapidly as a function of the neutron energy, and typical resonances can be observed, different from element to element. These values of σ cannot simply be predicted for a given element.

As already stated above, the resonances are mainly due to neutron capture (n, γ). Indeed, in this energy region one can say that normally $\Gamma_\gamma > \Gamma_n > \Gamma_p$ and Γ_α. It is easy to understand that Γ_p and Γ_α are small in this region, because resonance neutrons cannot sufficiently excite the compound nucleus to allow protons or α-particles to penetrate the Coulomb barrier around the nucleus. Sometimes, $\Gamma_n > \Gamma_\gamma$, particularly in the case of light nuclei and at somewhat higher neutron energy. The resonance phenomenon is then mainly due to scattering.

There are quite different forms of resonance, depending on the value of the resonance parameters (E_r and Γ). Some typical examples are represented in Figure 3.4, with special reference to the nuclide which is responsible for the resonance. The resonance parameters, corresponding to the data of Figure 3.4, are summarized in Table 3.3.

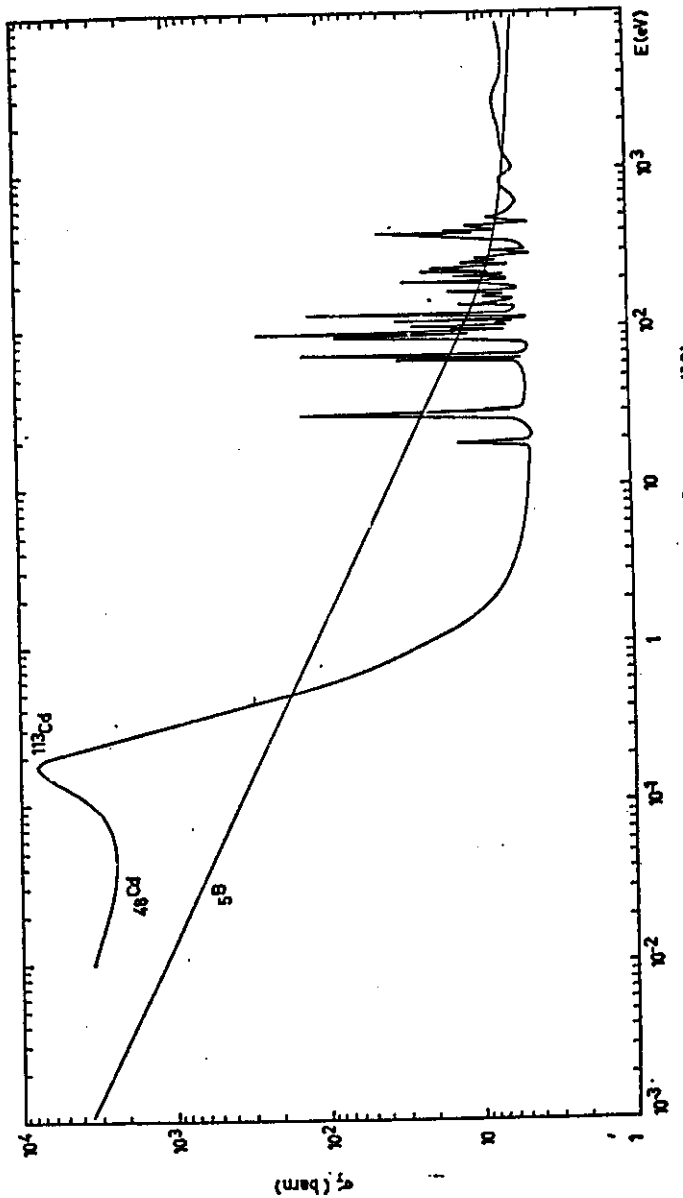

Fig. 3.4. Some typical forms of resonance (13).

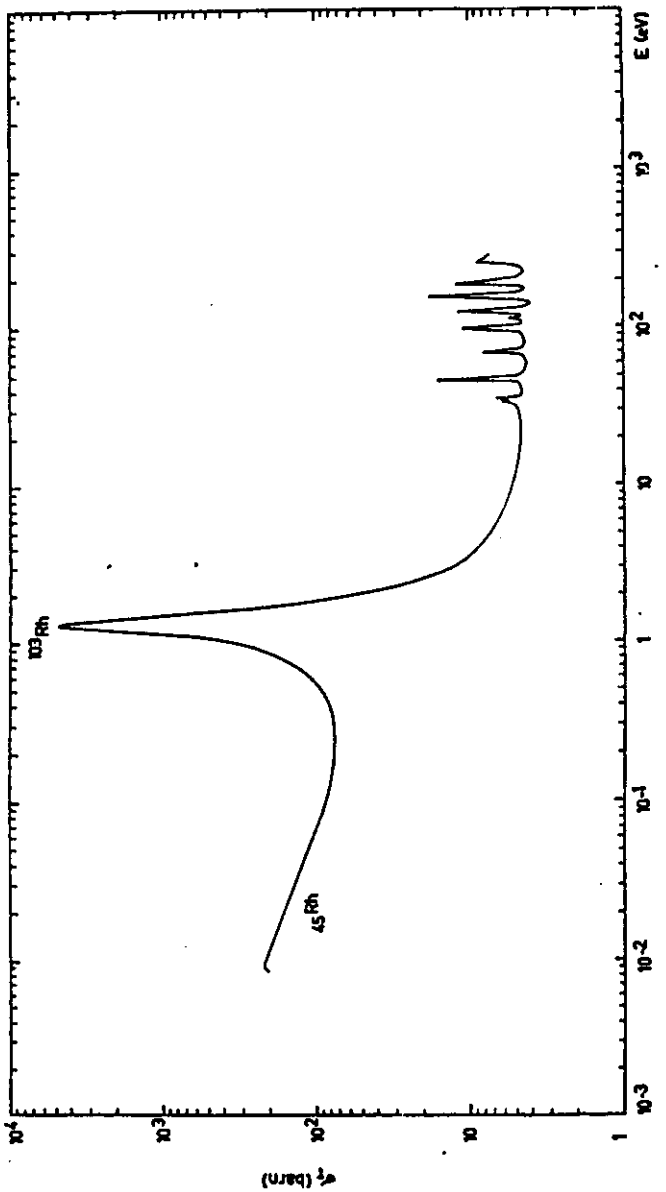

Fig. 3.4 *continued*

TABLE 3.3

Resonance parameters of the data of Figure 3.4 (13)

	Resonance energy	Level width	Remark
^{10}B	530 ± 30 keV	Γ_n = 100 ± 20 keV	$E_r \gg$ thermal energy
	1860 ± 20 keV	450 ± 50 keV	
	2800 keV	300 keV	
	4100 keV	500 keV	
^{11}B	430 ± 10 keV	Γ_n = 40 ± 5 keV	
	1280 ± 20 keV	140 ± 20 keV	
	1780 ± 20 keV	60 ± 20 keV	
	2450 ± 20 keV	120 ± 40 keV	
	2580 ± 20 keV	60 ± 20 keV	
^{113}Cd	0.178 ± 0.002 eV	Γ_γ = 113 ± 5 mV	E_r epitherm. energy
		(Γ_n = 0.65 ± 0.02 mV)	$\Gamma \approx E_r$
^{103}Rh	1.257 ± 0.002 eV	Γ_γ = 155 ± 4 mV	E_r epitherm. energy
		(Γ_n = 0.78 ± 0.01 mV)	$\Gamma \ll E_r$

(b) Resonance integral cross section. Obviously, a reaction rate in the intermediate neutron energy region can be calculated if the neutron energy distribution and the cross section curve $\sigma(E)$ are known. In the reactor (equation (4.15)) the intermediate neutron energy distribution is $\propto 1/E$. Hence

$$I_x = \int_{E_{Cd}}^{2\text{MeV}} \sigma_x(E)\,\frac{dE}{E} \approx \int_{E_{Cd}}^{\infty} \sigma_x(E)\,\frac{dE}{E} \qquad (3.21)$$

x represents the type of nuclear reaction (neutron absorption, activation, fission, etc.) and I_x is called (absorption, activation, fission, . . .) epicadmium resonance integral at infinite dilution. The definition of effective resonance integral (corrected for self-absorption) appears in equation (10.7). The lower limit of the above integral is the cadmium cut-off E_{Cd} (see Figure 3.4) and depends on the experimental conditions. The EANDC* recommends the value E_{Cd} = 0.55 eV in equation (3.21) (15). Some typical values for the effective cadmium cut-off energy in various geometries, calculated according to Stoughton (8) and Westcott (9,10), are given in Table 3.4.

* European American Nuclear Data Committee (15).

TABLE 3.4

Effective cadmium cut-off for 1/v absorbers (in eV) (12).

Cadmium thickness (mm)	Collimated neutron beam	Isotropic neutron flux density		
		Foil in Cd sandwich	Small sample in spherical shell	Small sample in cylindrical shell
0.76	0.473	0.62	0.476	0.50
1.02	0.512	0.68	0.518	0.55
1.52	0.567	0.77	0.583	0.62

The resonance integral I_s contains the resonance contribution, as well as the 1/v-tail (see Section V, C 1a). Indeed, in the case of a single resonance peak in the $\sigma(E)$ curve, the cross section in the resonance region can be divided into two parts:

a contribution $\sigma_r(E)$, ideally given by the Breit–Wigner formula;
a contribution $\sigma_{1/v}(E)$, due to the fact that, when no resonances are present, the cross section generally varies 1/v.

The equation:

$$\int_{E_C}^{\infty} \sigma(E)\frac{dE}{E} = \int_{E_{Cd}}^{\infty} \sigma_{1/v}(E)\frac{dE}{E} + \int_{E_{Cd}}^{\infty} \sigma_r(E)\frac{dE}{E}$$

is abbreviated as:

$$I = I_{1/v} + I' \tag{3.22}$$

Numerical values of I are given in Appendix 2, Table 1, after normalizing to a cadmium cut-off of 0.5 eV. Numerical values for I, I' and $I_{1/v}$ are separately listed for some interesting nuclides in Table 3.9.

Calculation of I'_s is possible if the resonance parameters (Γ_n, Γ_γ, Γ, E_r) and/or the 2200 m/s cross section are known. Several formulas are proposed in the literature, such as (12)

$$I'_{act} = (4.10 \times 10^6) g\Gamma_n\Gamma_\gamma/E_r^2\Gamma \tag{3.23}$$

where E_r is the resonance energy expressed in eV, and the Γ's are the level widths in eV; g is a statistical factor depending on the angular momentum of the compound nucleus. Another, less accurate formula is given by Dresner (16):

$$I'_{act} = 2\pi\sigma_0(E_0E_r)^{1/2}/\Gamma \tag{3.24}$$

where σ_0 is the activation cross section for 2200 m/s neutrons; E_0 = 0.025 eV and E_r and Γ are the neutron resonance energy and width for the resonance. If $\sigma_r(E_r)$, the total cross section at the maximum of the resonance is known, the following equation can be used (see Chapter 10, Table 10.3).

$$I'_{act} = \pi\Gamma_\gamma\sigma_r(E_r)/2E_r \tag{3.25}$$

The 1/v contribution depends obviously on the cadmium cut-off value (see Table 3.4). It can be shown that the expression

$$\int_{E_{Cd}}^{\infty} \sigma_{1/v}(E)\frac{dE}{E}$$

equals 0.90 σ_0; 0.45 σ_0; 0.424 σ_0 or 0.38 σ_0 for E_{Cd} = 5 kT; 0.50 eV; 0.55 eV; 0.68 eV respectively (12).

As will be shown further, the knowledge of I_{abs} is of interest to estimate neutron shielding effects in reactor positions, where the neutrons are not well thermalized. In section II, B, 4 of Chapter 10, some additional information will be given for the actual calculation of neutron shielding effects if the thermal cross section, the resonance integral and the thermal and resonance fluxes are known.

(c) Calculation of a reaction rate for reactor irradiation. If a nuclide is irradiated in a reactor neutron spectrum, both thermal and resonance activation are possible. Consequently, equation (3.17) must be adapted. The simplest approach has been proposed by Høgdahl (14). The reactor neutron spectrum is described as the sum of thermal neutrons (those that are absorbed by a cadmium filter, i.e. integrated from 0 to E_{Cd}) and epicadmium neutrons (those that are not absorbed by a cadmium filter, integrated from E_{Cd} to 1–2 MeV or to ∞). The reaction rate per atom can be represented by

$$R = \int_0^{\infty} n(v)v\sigma(v)\,dv = \int_0^{v_1} n(v)v\sigma(v)\,dv + \int_{v_1}^{\infty} n(v)v\sigma(v)\,dv$$

$$= \sigma_0 v_0 \int_0^{v_1} n(v)\,dv + \varphi_e \int_{E_{Cd}}^{\infty} \frac{\sigma(E)}{E}\,dE$$

or

$$R = n_{th}v_0\sigma_0 + \varphi_e I \tag{3.26}$$

where n_{th} = neutron density for energies up to the Cd cut-off

$$= \int_0^{v_1} n(v)\,dv;$$

v_1 corresponds to the cadmium cut-off energy E_{Cd}, e.g. 0.55 eV.

v_0 = 2200 m/s and σ_0 = 2200 m/s cross section; actually one should write here σ_{th} instead of σ_0. For most nuclides, however, σ_{th} approximates σ_0 very closely, nl. if the $1/v$ law is followed (see also section 1 of Chapter 10).

φ_e = epicadmium flux density per unit logarithmic energy interval ($>E_{Cd}$). Indeed, since in this energy region (e.g. E_1 to E_2), $\varphi(E) \propto 1/E$, nl. $\varphi(E) = \varphi_e/E$ the total intermediate flux density is given by

$$\varphi_{int} = \int_{E_1}^{E_2} \varphi(E)\,dE = \varphi_e \int_{E_1}^{E_2} dE/E = \varphi_e \ln(E_2/E_1).$$

Hence the quantity φ_e can be given the interpretation of an intermediate (or epicadmium) flux density per unit logarithmic energy interval.

I = the infinite dilute (epicadmium) resonance integral =

$$\int_{E_{Cd}}^{1\,MeV} \frac{\sigma(E)}{E}\,dE;$$

$I = I' + I_{1/v} = I' + 0.45\,\sigma_0$ for a cadmium foil thickness of ca. 1 mm.

The reason for ignoring the presence of a fission spectrum in equation (3.26) is that the contribution to the total (n, γ) reaction due to fission neutrons is usually very small.

The form of equation (3.17) can be conserved, if σ_0 is replaced by a "reactor" cross section $\sigma_{reactor}$:

$$R = n_{th} v_0 \sigma_{reactor} \tag{3.27}$$

where

$$\sigma_{reactor} = \sigma_0 + \frac{\varphi_e}{n_{th} v_0} I \tag{3.28}$$

and $n_{th}v_0 = \varphi_{th}$ (conventional thermal flux for neutron energies $\leq E_{Cd}$).

Equation (3.27) allows the calculation of the reaction rate (induced activity) if φ_{th} and φ_e/φ_{th} are known. In Section VI, B of this chapter a method is described for determining these quantities. Numerical

data for σ_0 and I are given in Appendix 1, Table 2, and Appendix 2, Table 1.

For practical use in activation analysis, reference is made to equation (10.1), which takes into account the weight of the irradiated element, the irradiation time and the half-life of the product radionuclide.

Note that for a pure $1/v$-absorber (no resonance peaks, $I' = 0$), equation (3.26) is reduced to

$$R = n_{th} v_0 \sigma_0 + 0.45 \varphi_e \sigma_0 = n_{th} v_0 \sigma_0 (1 + 0.45 \varphi_e / n_{th} v_0)$$

The reaction rate is also given by equation (3.17):

$$R = n v_0 \sigma_0$$

where n = total neutron density ($0 \rightarrow \infty$).

Hence: $n = n_{th}(1 + 0.45\varphi_e/n_{th}v_0)$

As for most irradiation positions $\varphi_e/n_{th}v_0 < 1/10$, one can conclude that the first term on the right hand in equation (3.26) is practically equal to equation (3.17) and takes the thermal activation almost completely into account.

3. *Fast neutrons* (>1 MeV)

(a) 14 MeV neutrons (neutron generator). The behavior of σ will be considered for 14 MeV neutrons, as this energy region is of great interest for activation analysis with a neutron generator, using the T(d, n)α reaction (see Chapter 4, II).

(1) σ_T. For 14 MeV neutrons, σ_T can easily be calculated for a given element; this was not possible for thermal, epithermal and resonance neutrons. The following equation holds:

$$\sigma_T = 2\pi R_A^2 \tag{3.29}$$

where the nuclear radius R_A is correlated with the atomic mass number A by the approximate relationship

$$R_A \simeq 1.5 \times 10^{-13} A^{1/3}\ \text{cm} \tag{3.30}$$

This means that $\sigma_T^{1/2}$ is proportional with $A^{1/3}$ and that for all elements σ_T has a value between 1.5 and 6 barn at a neutron energy of 14 MeV.

Example: Hg. Calculated $\sigma_T = 2\pi \times 2.25 \times 10^{-26} \times (201)^{2/3}\ \text{cm}^2 = 4.85$ b.

Experimental value at $\sim$14 MeV = 4.5–5.2 barn.

Equation (3.29) seems to be contrary to the definition of cross section by equation (3.10), due to the factor 2. This can be explained as follows: the probability for the formation of a compound nucleus is indeed given by πR_λ^2, but the total cross section includes an additional πR_λ^2 for diffraction scattering, which does not produce a compound nucleus (see last two columns of Table 3.5). Anyway, the correspondence between the experimental σ_T values and those, calculated by equation (3.29) indicates that at higher neutron energy the nucleus may be considered as a non-transparent sphere and the neutrons as simple projectiles and that σ_T is directly correlated with the geometrical dimensions of the nucleus. This σ_T can be regarded as a sum of the probabilities for elastic and non-elastic (in many cases = inelastic) scattering (*cf.* this chapter, section 1. Within the scope of this book, no distinction will be made between σ_{inel} and $\sigma_{n.e.}$).

$$\sigma_T = \sigma_{el} + \sigma_{n.e.} \tag{3.31}$$

where

$$\sigma_{n.e.} = \sigma(n, 2n) + \sigma(n, p) + \sigma(n, \alpha) + \sigma(n, \gamma) + (n, n\alpha) \ldots \tag{3.32}$$

The numerical value of $\sigma_{n.e.}$ for 14 MeV neutrons can be calculated by the following empirical formula (17)

$$\sigma_{n.e._{(14\,MeV)}} = \pi\,(0.12A^{1/3} + 0.21)^2 \text{ barn} \tag{3.33}$$

The calculated value for Al is 1.02 barn, whereas the experimental value (13) is 0.99 barn.

(2) $\sigma(n, \gamma)$. At 14 MeV, the probability for a (n, γ) reaction is small. The most important phenomena are elastic scattering and inelastic collision followed by (n, 2n), (n, p) and (n, α) reactions. (Table 3.5). σ_T and $\sigma_{n.e.}$ can be calculated empirically by equations (3.29), (3.30) and (3.33).

Anyhow, the relative importance of the (n, γ) reaction decreases very rapidly with increasing neutron energy (Figure 3.5). For that matter its value at 14 MeV is normally determined by linear extrapolation in the log σ vs. log E_n plot (Figure 2.5, Ref. (18)).

(3) $\sigma(n, 2n)$. At 14 MeV other reactions are favored, particularly (n, 2n) reactions, as can be seen from Table 3.5. In most cases $\sigma(n, 2n) \approx \sigma_{n.e.}(\approx \frac{1}{2}\sigma_T$ or $\approx \pi R_\lambda^2)$. (*Cf.* equation (3.32) and this section 3, a(1) respectively).

Obviously, the cross section for (n, 2n) reactions will depend on the relative excess of neutrons in the target nucleus. A second neutron can, of course, leave the nucleus more easily, if the neutron excess is greater. As a measure for the neutron excess one normally chooses $(N-Z)/A$, where N = number of neutrons, Z = number of protons, $A = N + Z$ = mass number.

TABLE 3.5
Some 14 MeV neutron cross sections (mb).

Isotope	$\sigma(n, \alpha)$	$\sigma(n, p)$	$\sigma(n, 2n)$	$\sigma(n, \gamma)$	$\sigma_{n.e.}$(element)	σ_T(element)
^{197}Au	0.5	2.4	2600	7.6	2600	5200
^{209}Bi	0.5	0.95	2400 (tot)	1.5	2500	5600
^{107}Ag	(10)	(22)	I 550 (24.5m) II 600 (8.3d)	30	1800	4300
^{109}Ag	10	13	600	...		
^{75}As	12	12	540	2	...	...
^{63}Cu	(37)	120	520	2.6	1500	2950
^{65}Cu	(13)	19	1000	6		

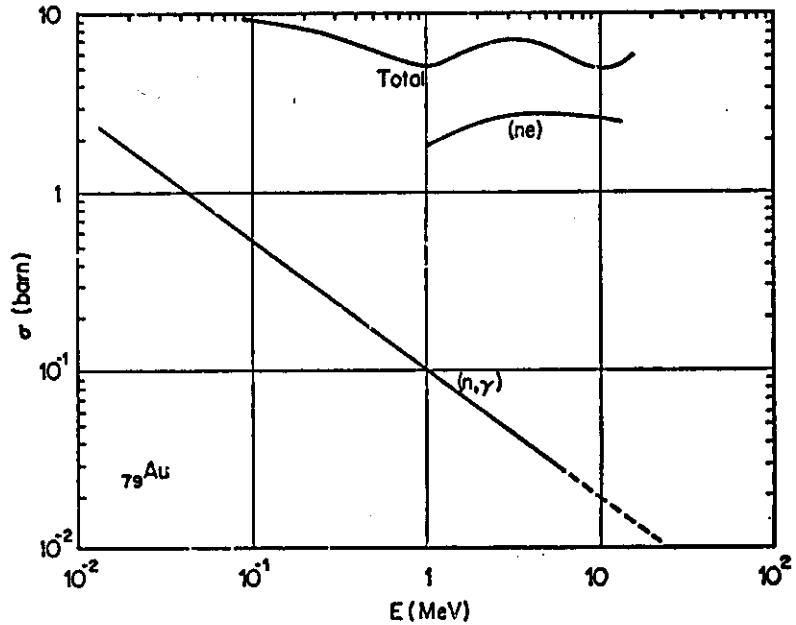

Fig. 3.5. σ_T, $\sigma_T - \sigma_{el} = \sigma_{n.e.}$ and $\sigma(n, \gamma)$ for $_{79}$Au at higher neutron energy (13).

The following empirical relationship between $\sigma(n, 2n)$ and $(N - Z)/A$ is valid:

For $(N - Z)/A > 0.07$:

$$\log \sigma(n, 2n)_{(14\ MeV)} = 2.473 + 3.48 \frac{N - Z}{A} (mb) \qquad (3.34)$$

For $(N - Z)/A < 0.07$:

$$\log \sigma(n, 2n)_{(14\ MeV)} = -0.341 + 42 \frac{N - Z}{A} (mb) \qquad (3.34\ bis)$$

This relationship holds as well for odd–even as for even–even nuclei.

Example: $^{123}Sb(n, 2n)^{122(m)}Sb$, $Z = 51$, $A = 123$, $N = 72$, $(N - Z)/A = 0.171$.

From equation (3.34) one calculates $\sigma(n, 2n)_{(14\ MeV)} = 1162$ mb.

Experimental value: $\sigma(n, 2n)_{(14.0\ MeV)} = 1560$ mb.

Experimental values of $\sigma(n, 2n)$ for 14 MeV neutrons are given by Friedlander and Kennedy (1), Neuert and Pollehn (19) and W. Schulze (18); see Appendix 4, Table 3. Schulze (18) gives also calculated values if no experimental data are available. Determining $\sigma(n, 2n)$ experimentally, one often uses the reaction $^{63}Cu(n, 2n)^{62}Cu$ as a reference ($\sigma = 500$ mb, ± 5 to 8% at $E_n = 14.1$ MeV). (Figure 3.6).

If $\sigma(n, 2n)$ is plotted vs. the neutron energy, a so-called excitation function is obtained; (n, 2n) reactions are, of course, threshold reactions, as at least the binding energy of 1 neutron must be available. At increasing neutron energy, the reaction yield increases too and a smooth continuous function of energy is obtained. However, at a sufficient high neutron energy the yield of the (n, 2n) reaction can decrease, owing to competing reactions, which become more favored. An analogous phenomenon was already observed for (n, γ) reactions at energies >0.1–1 MeV, see above, Figure 3.5. A typical excitation function is represented in Figure 3.6.

(4) $\sigma(n, p)$ *and* $\sigma(n, \alpha)$. (n, p) and (n, α) reactions are normally threshold reactions too, and similar excitation functions are obtained (Figures 3.16, 3.17).

Some numerical values of such a curve are of particular interest, nl. $\sigma_{(14MeV)}$ and σ_{max}; for the reaction $^{27}Al(n, \alpha)\ ^{24}Na$, σ_{max} is at ca. 14 MeV. There exist empirical relationships which allow the approximate calculation of $\sigma(n, p)$ and $\sigma(n, \alpha)$ in the 14 MeV region (21). The ratios $\sigma(n, p)$, resp. $\sigma(n, \alpha)$ to $\sigma_{n.e.}$ are correlated by the same

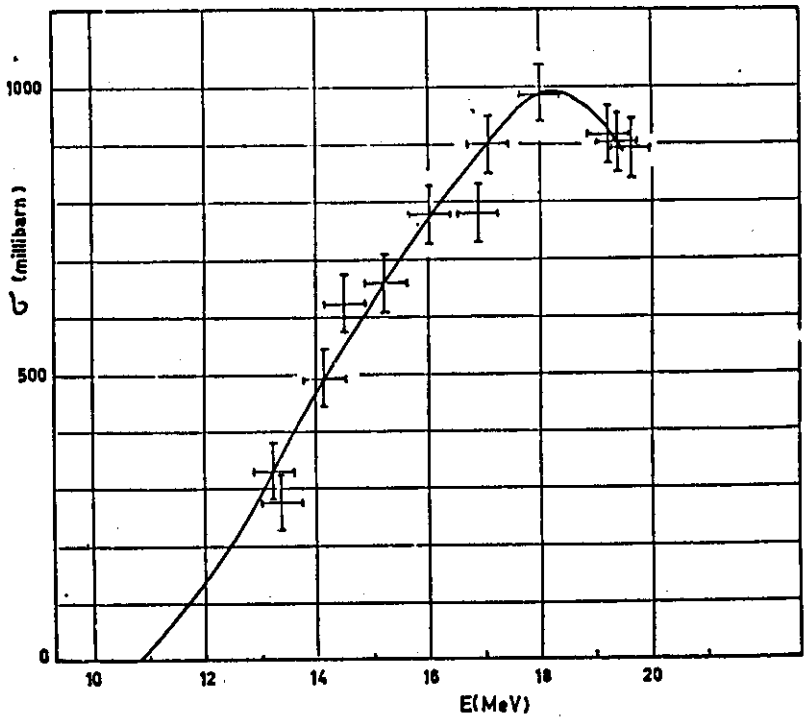

Fig. 3.6. Energy dependence of the reaction cross section for $^{63}Cu(n,2n)^{62}Cu$ (20).

parameter $(N - Z)/A$, which was already introduced in equation (3.34).

The maximal $\sigma(n, p)$ is given by:

$$\frac{\sigma(n, p)_{max}}{\sigma_{n.e.}} = k \exp\left(-25.2 \frac{N - Z}{A}\right) \qquad (3.35)$$

where k(o.–e.) = 0.28 and k(e.–e.) = 0.47.

This means, that the behavior of odd–even (o.–e.) and even–even (e.–e.) is not the same. For even–odd nuclei, no sufficient data are available. $\sigma_{n.e.}$ is calculated by equation (3.33).

At 14 MeV, $\sigma(n, p)$ is given by

$$\frac{\sigma(n, p)_{(14\ MeV)}}{\sigma_{n.e.}} = k \exp\left(-31.1 \frac{N - Z}{A}\right) \qquad (3.36)$$

where k(o.–e.) = 0.50 and k(e.–e.) = 0.83.

Example: $^{106}Ag(n, p)^{106}Pd$
Experimental value: $\sigma(n, p)_{(14\ MeV)} = 13$ mb
Calculated: $A = 109$, $Z = 47$, $N = 62$, $\sigma_{n.e.} = 1.96$b, $\sigma(n, p)_{(14\ MeV)} = 11.2$ mb.

Similar relationships are formulated for (n, α) reactions:

$$\frac{\sigma(n, \alpha)_{(max)}}{\sigma_{n.e.}} = k \exp\left(-37.7 \frac{N - Z}{A}\right) \tag{3.37}$$

where k(o.–e.) = 0.55 and k(e.–e.) = 0.92.

$$\frac{\sigma(n, \alpha)_{(14\ MeV)}}{\sigma_{n.e.}} = k \exp\left(-37.8 \frac{N - Z}{A}\right) \tag{3.38}$$

where k(o.–e.) = 0.50 and k(e.–e.) = 0.83.

Considering the parameters in equations (3.37) and (3.38) one can expect that in most cases σ(n, α) will be maximum at ~14 MeV, as can be seen from Figure 3.16.

Experimental values of σ(n, p) and σ(n, α) for 14 MeV neutrons are tabulated by Friedlander and Kennedy (1), Neuert and Pollehn (19) and Schulze (18), see Appendix 4, Tables 1–2. The latter author gives also calculated values if experimental data are lacking. Some selected reactions are often used for relative comparative measurements, e.g.

$^{6}Li(n, \alpha)^{3}H$ $\sigma_{(14.1\ MeV)} = 26$ mb (± 5 to 8%)

$^{27}Al(n, \alpha)^{24}Na$ $\sigma_{(14.1\ MeV)} = 121$ mb (± 3%)

$^{27}Al(n, p)^{27}Mg$ $\sigma_{(14.1\ MeV)} = 81$ mb (± 5 to 8%)

(5) *Other reactions.* It must be borne in mind that with 14 MeV neutrons not only (n, 2n), (n, p), (n, α) and (n, γ) reactions are possible, but also

(n, n')
(n, np + n, pn + n, d)
(n, p + n, pn)
(n, np) or (n, nd)
(n, d) or (n, ^{3}He)
(n, p + n, pn + n, np + n, d)
(n, t) or (n, 2p) or (n, tn)
(n, nα) reactions

Experimental data are given in Ref. 19.

Some (n, n') reactions, produced in the reactor, are discussed in section V, C, 3b of this chapter.

(6) *Calculation of the reaction rate for accelerator irradiation.* The reaction rate per atom is given by

$$R_{14\ MeV} = F \cdot \sigma_{14\ MeV}(s^{-1}) \tag{3.39}$$

where σ = the 14 MeV neutron cross section for the reaction of interest (see Appendix 4);
F = the 14 MeV neutron flux (see Section VI, B, 4 of this chapter).

For practical use in activation analysis, reference is made to equation (10.1), which allows the calculation of the induced activity, taking into account the weight of the irradiated element, the irradiation time and the half-life of the product radionuclide.

(b) Fission neutrons (Reactor)

(1) *Definition of average cross section* ($\bar{\sigma}$) *for a fission neutron flux.* Contrary to the neutron generator, reactor neutrons are not monoenergetic. According to Watt (22), neutrons produced by fission of ^{235}U have the following energy distribution (Figure 3.7):

$$f(E) = C \exp(-E) \sinh \sqrt{(2E)} \tag{3.40}$$

where E is expressed in MeV; for the normalized distribution $C = 0.484$.

Cranberg (23) proposed the following modification

$$f(E) = 0.4527 \exp(-1.036E) \sinh \sqrt{(2.29E)} \tag{3.40 bis}$$

Another semiempirical expression has been proposed by Leachman (24):

$$f(E) = 0.7725\, E^{1/2} \exp(-0.775\, E) \tag{3.40 tris}$$

Equation (3.40) agrees with the experimental data from 0.075 to 15 MeV; equation (3.40 bis) has been studied experimentally from 0.18 to 12 MeV; equation (3.40 tris) is a good approximation for the fission spectrum <9 MeV. These representations differ only slightly, the largest deviations occurring at high energies. For in-pile measurements this neutron spectrum is mostly slightly disturbed above 1–3 MeV, although departure from this distribution is possible.

As already stated, the cross section for a threshold reaction is energy dependent (excitation curve). In the case of emission of a charged

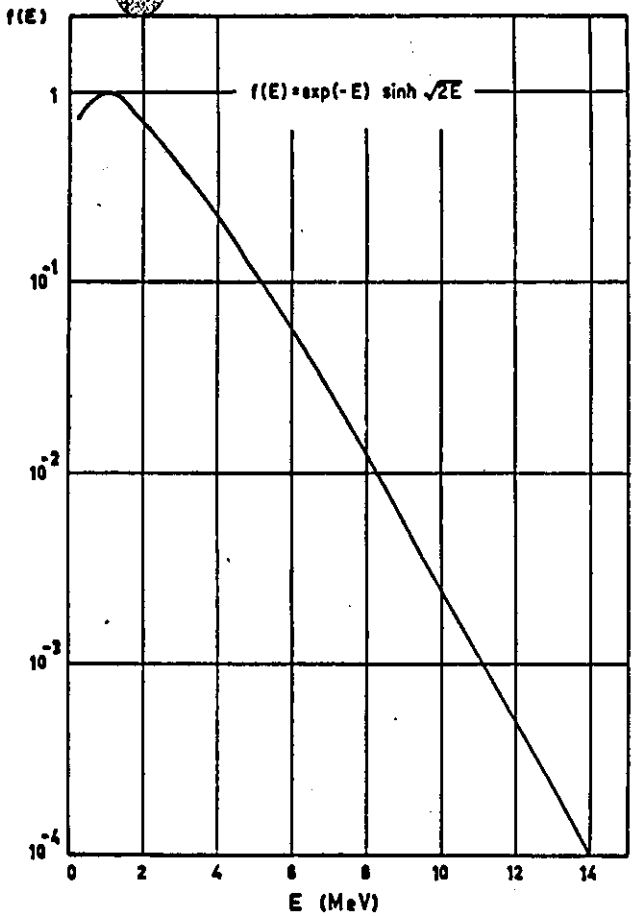

Fig. 3.7. Energy distribution of fission neutrons from ^{235}U (Watt distribution) (2). (Permission of Hughes, D. J., *Pile Neutron Research*, 1953, Adison-Wesley, Reading, Mass.)

particle (p or α) this excitation function is mainly determined by the penetrability of the potential barrier around the nucleus (2). It is 0 for $E \leqslant E_T$ and increases with the neutron energy. It can decrease again due to competing reactions or because the nucleus becomes transparent (*cf.* Figures 3.6, 3.16, and 3.17). At any energy the reaction rate is given by the response function $\sigma(E)f(E)$. The integral reaction rate per second and per target nucleus is given by

$$\int_0^\infty \sigma(E)f(E)\,dE = \int_{E_T}^\infty \sigma(E)f(E)\,dE \text{ (as } \sigma = 0 \text{ for } E < E_T) \quad (3.41)$$

This quantity is called the response integral. In fact it is this response integral which results directly from measurements with activation detectors. $f(E)$ represents the fraction of the fission neutron flux between E and $E + dE$. Equation (3.41) is equivalent with $\bar{\sigma}\int_0^\infty f(E)\,dE$ if $\bar{\sigma}$ is the average cross section in a fission neutron spectrum; $\bar{\sigma}$ is thus defined as follows:

$$\bar{\sigma} = \frac{\int_0^\infty \sigma(E)f(E)\,dE}{\int_0^\infty f(E)\,dE} = \frac{\int_{E_T}^\infty \sigma(E)f(E)\,dE}{\int_0^\infty f(E)\,dE} \quad (3.42)$$

$\int_0^\infty f(E)\,dE$ is mostly normalized to one neutron $cm^{-2}s^{-1}$. In practice it is $\bar{\sigma}$, that for a given reaction is determined in an unperturbed fission neutron spectrum, as the response is automatically integrated over the whole spectrum. Obviously $\bar{\sigma}$ can, in principle, also be calculated if the energy distribution of the flux and the excitation function $\sigma(E)$ of the reaction of interest are known (see Section VI of this chapter).

The definition of σ_{eff} is given by equation (3.5). From equation (3.5) and (3.42) it follows that

$$\frac{\bar{\sigma}}{\sigma_{eff}} = \frac{\int_{E_{eff}}^\infty f(E)\,dE}{\int_0^\infty f(E)\,dE} \quad (3.43)$$

Some "reduced" cross section curves ($\sigma(E)/\sigma_{eff}$ *vs.* E) are represented in Figures 3.16 and 3.17.

(2) (n, p) and (n, α) *reactions*. Hughes (2) described a relation between $\bar{\sigma}$ for (n, p) or (n, α) reactions and the fission integral $\int_{E_{eff}}^\infty f(E)\,dE$ (see Figure 3.8); $\bar{\sigma}$ was normalized to a "standard size nucleus".

This approach is, however, not completely justified and important discrepancies between experimental and expected values are observed. Roy and Hawton (25) proposed another empirical correlation between $\bar{\sigma}$ and E_{eff} (Figures 3.9 and 3.10), taking into account a larger number of recent experimental data, and normalizing to a standard nucleus with $A = 125$. (Indeed, σ is function of A, as can be seen from equations (3.29) and (3.30): $\sigma \propto A^{2/3}$; if $A = 125$ is arbitrarily chosen as the standard nucleus, it is obvious that any other $\bar{\sigma}$ has to be multiplied by a factor $(125/A)^{2/3} = 25/A^{2/3}$). Plotting $25\bar{\sigma}/A^{2/3}$ versus E_{eff} for (n, p) reactions, they find a different behavior for "odd-A" and

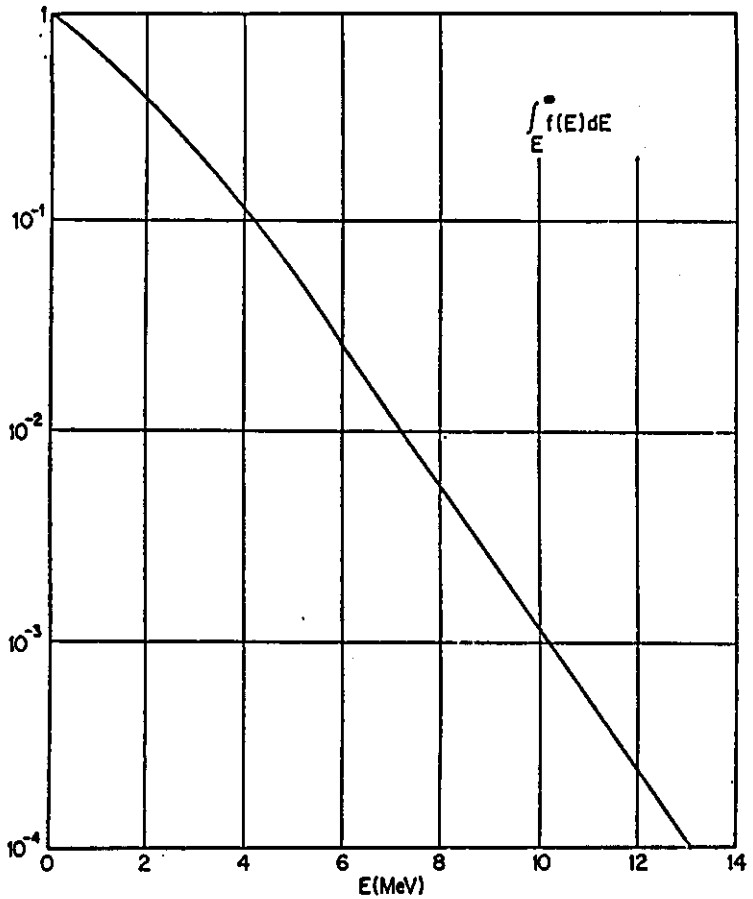

Fig. 3.8. Integral of the neutron fission spectrum.

"even-A" targets. The best fit through the experimental points gives straight lines, of which the slope apparently differs from that of the fission integral $\int_E^\infty f(E)\,dE$ versus E. $\bar{\sigma}$(n, p) for even-A nuclei is found to be about seven times that for odd-A nuclei (see Figure 3.9).

For (n, α) reactions the best fit also does not coincide with the integral of the fission spectrum (see Figure 3.10). However, significant differences for even-A and odd-A nuclei cannot be observed.

From these graphs, the $\bar{\sigma}$ for a given (n, p) or (n, α) reaction can be

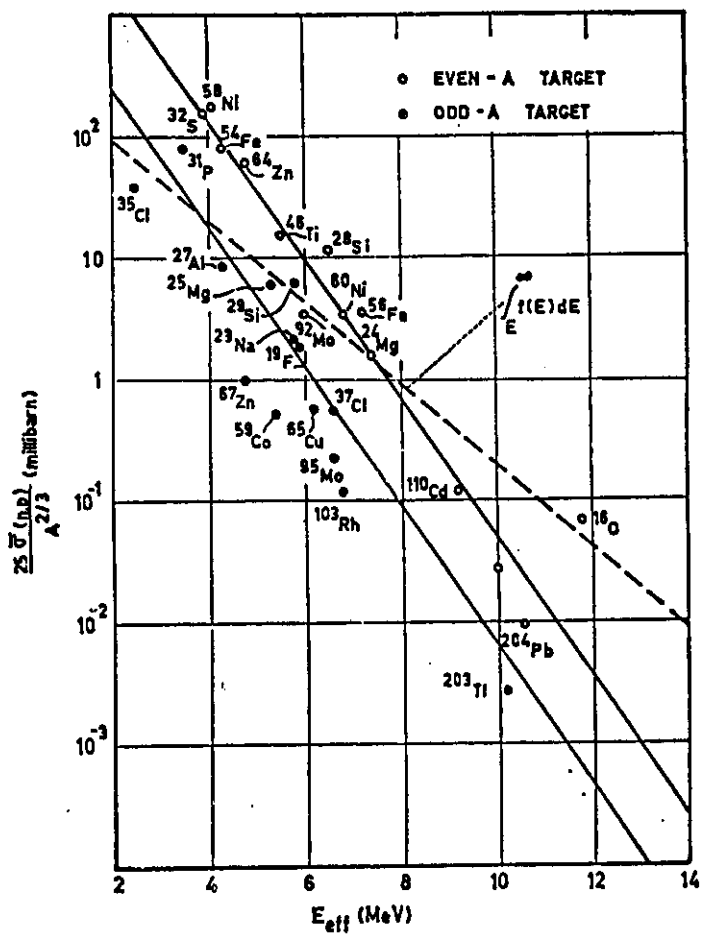

Fig. 3.9. Measured values of $\bar{\sigma}$(n, p) for fission neutrons, plotted vs. E_{eff} taken from Roy and Hawton (25). The dotted line represents the integral of the fission neutron spectrum.

estimated. First, E_T is calculated from the Q-value, using equation (3.4) or (3.6). E_{eff} can then be found from Figure 3.11, where $E_{eff} - E_T$ is plotted as a function of the atomic number of the target nucleus. Numerical data for E_{eff} can also directly be found in Ref. 25 or 11. From Figure 3.9 or 3.10 one estimates $25\bar{\sigma}/A^{2/3}$ and finally one calculates $\bar{\sigma}$.

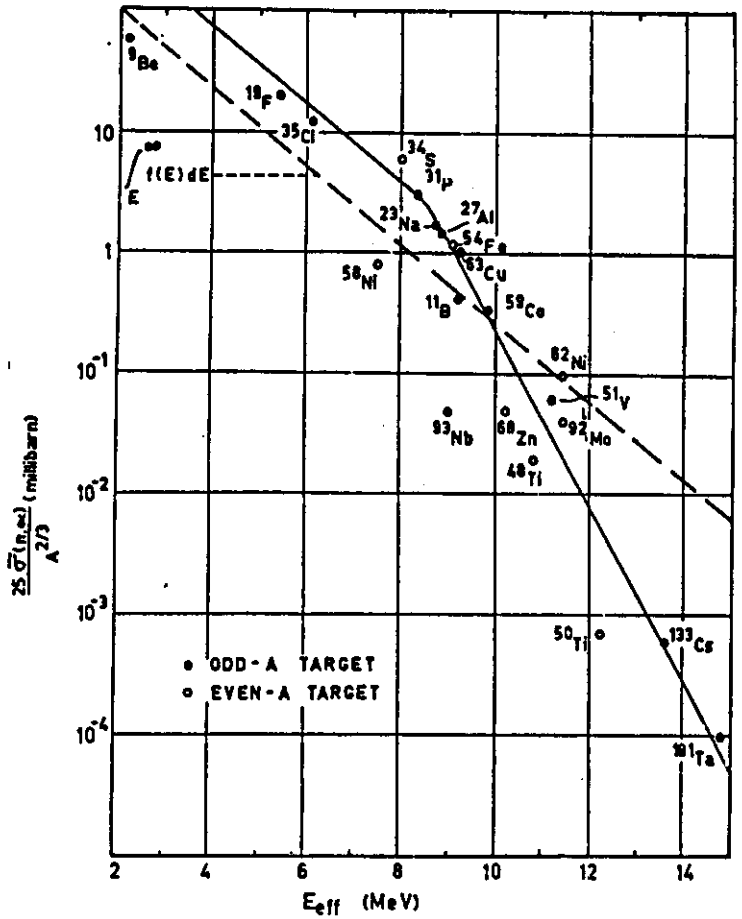

Fig. 3.10. Measured values of $\bar{\sigma}$(n, α) for fission neutrons, plotted vs. E_{eff}, taken from Roy and Hawton (25). The dotted line represents the integral of the fission neutron spectrum.

Using this method, discrepancies by a factor of 3 to 8 between experimental and estimated value are still observed. For that reason, De Neve (26) proposed to estimate $\bar{\sigma}$ for (n, p) and (n, α) reactions from the corresponding 14 MeV cross sections, where more experimental data are available (see Appendix 4).

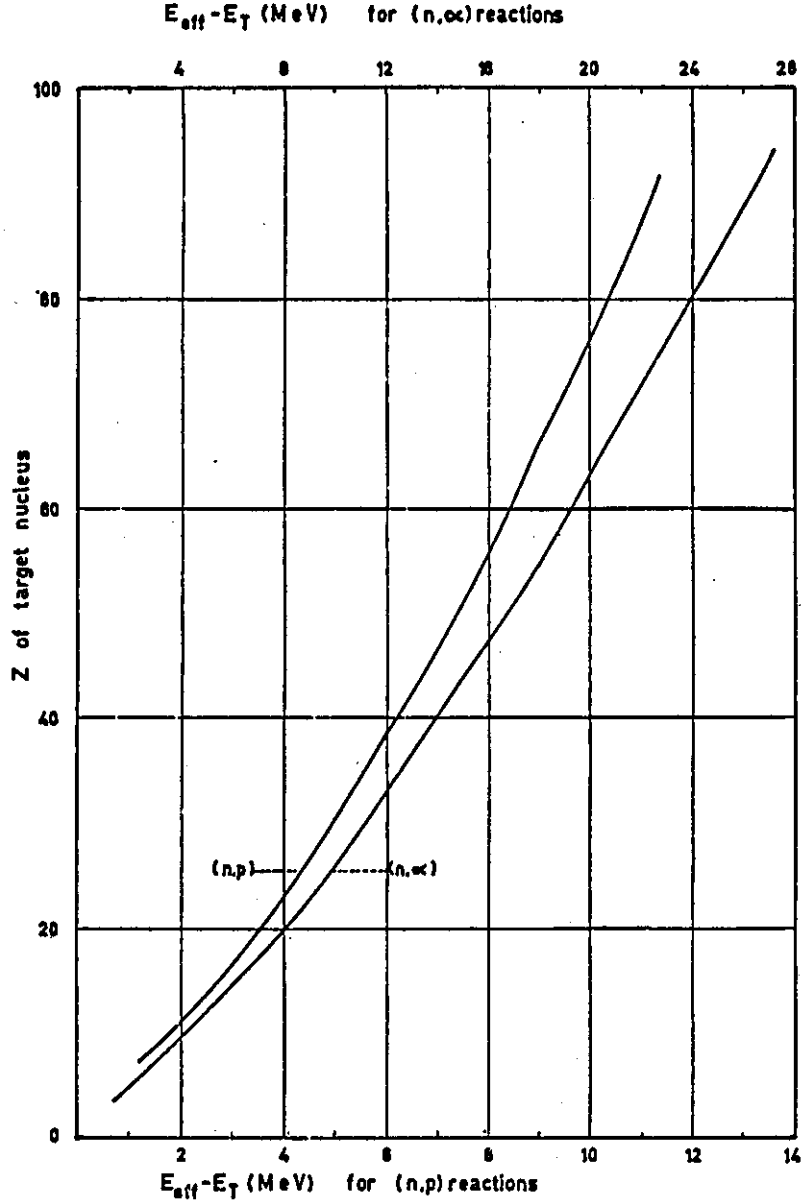

Fig. 3.11. The quantity $E_{eff}-E_T$ for (n, p) and (n, α) reactions as a function of the atomic number of the target nucleus, taken from Hughes (2). (Permission of Hughes, D. J., *Pile Neutron Research*, 1953, Adison-Wesley, Reading, Mass.)

In a normalized fission neutron flux $\int_0^\infty f(E)\,dE = 1$, equation (3.43) can be written as

$$\bar{\sigma}/\sigma_{\text{eff}} = \int_{E_{\text{eff}}}^\infty f(E)\,dE \qquad (3.44)$$

i.e. the fission integral, which is represented in Figure 3.8. σ_{eff} is the reaction cross section for a penetrability = 1. As seen in section V, C, 3a (4) of this chapter, the penetrability for most (n, p) and (n, α) reactions equals 1 at neutron energies $\simeq$ 14 MeV. Hence, equation (3.44) can be approximated as follows:

$$\bar{\sigma}/\sigma_{14\text{ MeV}} = \int_{E_{\text{eff}}}^\infty f(E)\,dE \qquad (3.45)$$

This relation is valid for (n, p) and (n, α) reactions and no different behavior is observed for odd-A or even-A target nuclei (Figure 3.12). From this Figure, $\bar{\sigma}$ can be estimated if $\sigma_{14\text{ MeV}}$ and E_{eff} (see above) are known; $\sigma_{14\text{ MeV}}$ can be found in Appendix 4, or estimated from the empirical relationships (3.36) or (3.38) and (3.33). In most cases, the difference between estimated and experimental values is not larger than a factor 3.

Numerical data for $\bar{\sigma}$(n, p) and $\bar{\sigma}$(n, α) can be found in Appendix 3.

(3) (n, 2n) *reactions*. Less experimental data are available for (n, 2n) reactions in a fission neutron spectrum. A plot of $25\bar{\sigma}(n, 2n)/A^{2/3}$ vs. E_T is represented in Figure 3.13. The choice of E_T instead of E_{eff} as a variable is justified as the quantity $E_{\text{eff}}-E_T$ does not vary by more than 1–2 MeV over the whole range of nuclides. This was not the case for (n, p) or (n, α) reactions, as appears from Figure 3.11. Moreover, E_T is a more accessible quantity than E_{eff}. The best fit through the experimental points yields again a straight line with another slope than $\int_E^\infty f(E)\,dE$. No systematic difference is observed for even-A and odd-A targets from the experimental data available.

Numerical data for $\bar{\sigma}$(n, 2n) are given in Appendix 3, Table 3.

As already stated in section V, C, 3a (2), (n, γ) reactions are unimportant for fast neutrons (*cf.* Figure 3.5 and Table 3.5).

(4) (n, n') *reactions–inelastic scattering*. Attention has been paid to the study of (n, n') reactions in reactor spectra. A few $\bar{\sigma}$(n, n') values have been determined (see Appendix 3, Table 4) but no empirical rules have been proposed.

Neutrons of ~0.1 to a few MeV can undergo inelastic scattering with a nucleus. The neutron loses its energy partly or completely,

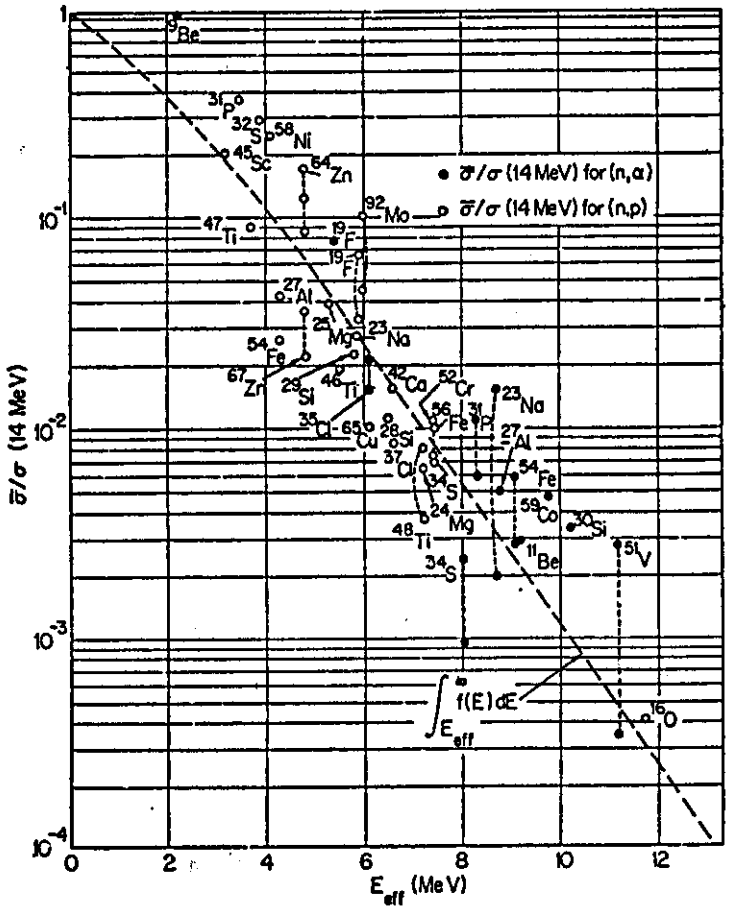

Fig. 3.12. Measured values of $\bar{\sigma}/\sigma$(14 MeV) for (n, p) and (n, α) reactions vs. E_{eff}, taken from De Neve (26). The dotted line represents the integral of the fission neutron spectrum.

leaving the nucleus in an excited state. Returning to the ground state, the nucleus emits one or more γ-rays. These so-called (n, n') reactions are also threshold reactions. Indeed, if the "lowest excited" state of the nucleus lies for instance at 850 keV above the ground state, it is obvious that the incident neutron must have at least an energy of 850 keV to make possible that particular (n, n') reaction, followed by emission of γ-radiation of 850 keV (as one γ-ray, or more γ-rays in

cascade). Plotting $\sigma(E)$ vs. E, one will again obtain an excitation function.

Examples.

( ) ^{56}Fe; isotopic abundance θ = 91.68%; energy levels 0, 845, 2080,

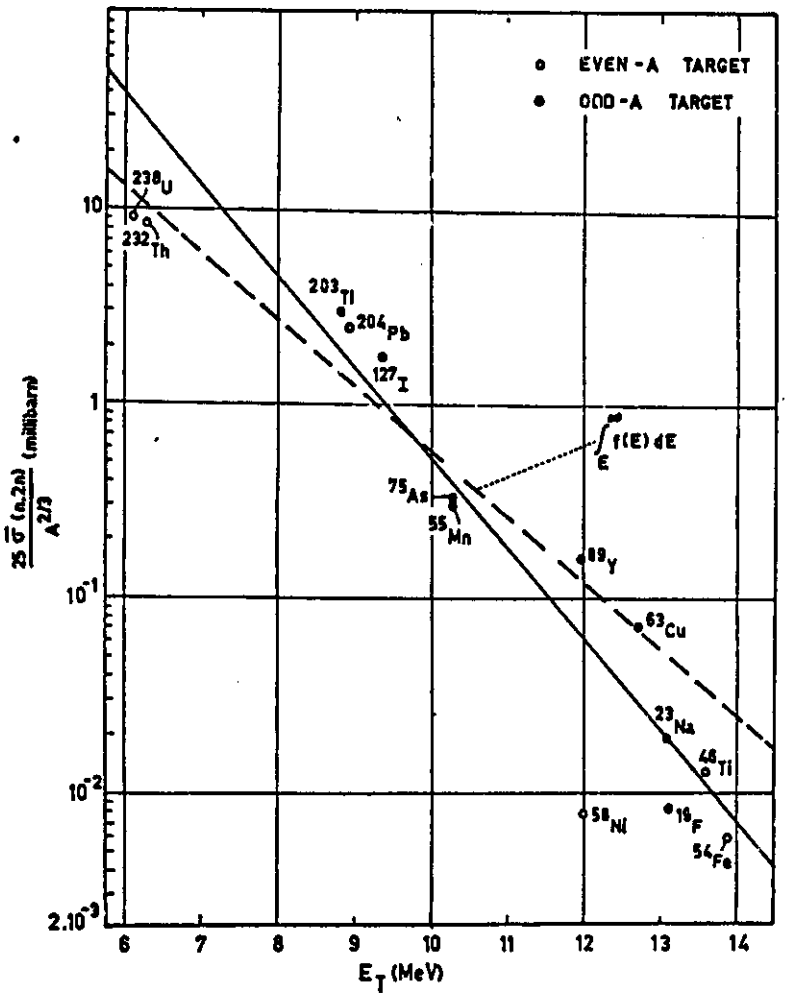

Fig. 3.13. Measured values of $\bar{\sigma}$(n, 2n) for fission neutrons, plotted vs. E_T, taken from Roy and Hawton (25). The dotted line represents the integral of the fission neutron spectrum.

2600, . . . keV. With neutrons from ca. 850 keV inelastic scattering produces γ-rays of 845 keV.

(2) ^{27}Al; θ = 100%; energy levels: 0, 834, 1015, 2270 keV. With neutrons from ca. 0.35 MeV, 1.02 MeV and 2.25 MeV one observes γ-rays of 0.847, 1.025 and 2.23 MeV. The excitation functions for these (n, n') reactions and the energy levels of ^{27}Al are represented in Figure 3.14. Data are taken from Hughes (13) and Dzhelepov (27).

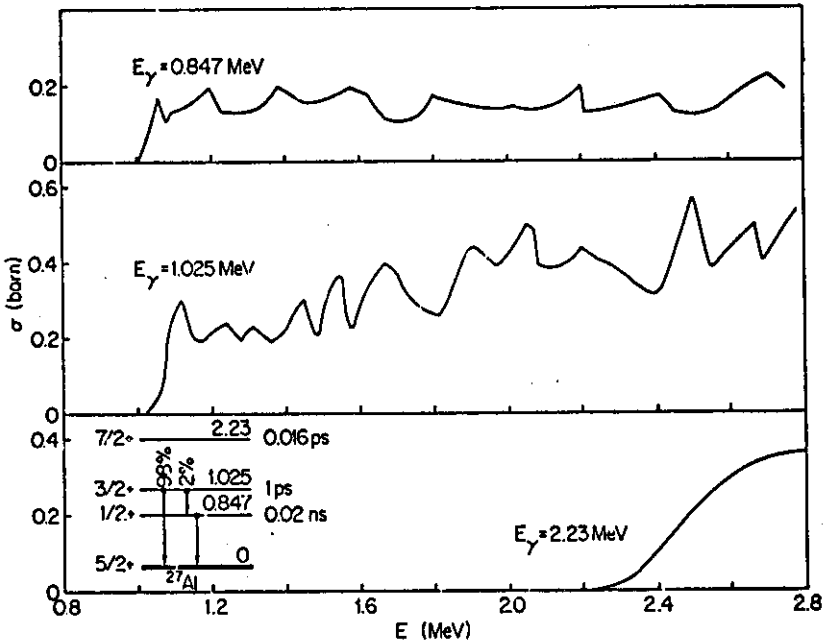

Fig. 3.14. Production of γ-rays by inelastic scattering and energy levels in ^{27}Al.

This type of reaction may be of analytical interest if a stable isotope gives an isomeric state of suitable half-life.

Example. ^{207}Pb; θ = 22.6%; energy levels 0, 565, 1633 keV. With neutrons from ca. 1.6 MeV ^{207m}Pb is formed ($T_{1/2}$ = 0.8 s) which decays to the ground state by emission of two γ-rays in cascade (1060 and 565 keV), see Figure 3.15 (taken from ref. 28).

Some other examples are summarized in Table 3.6.

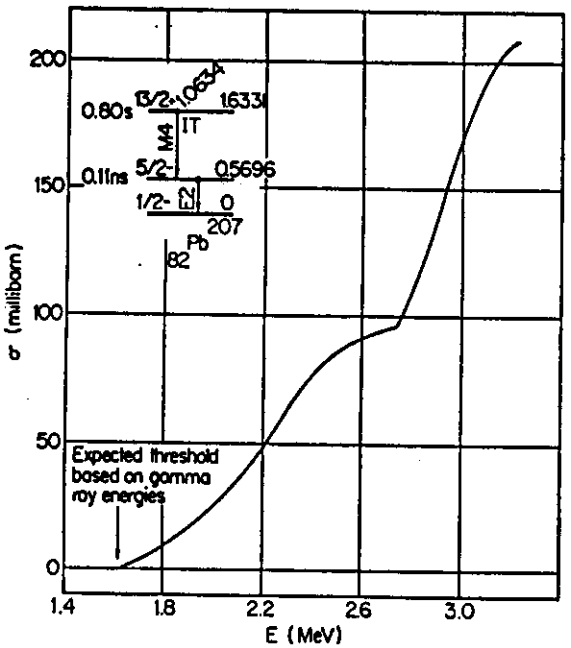

Fig. 3.15. Production of 0.8 s isomer ($^{207}Pb^{m}$) by inelastic scattering and energy levels in ^{207}Pb (partly).

TABLE 3.6
Production of isomers with measurable half-lives by inelastic neutron scattering

Reaction	θ %	$T_{1/2}$	E_γ (keV)	Threshold E_x (keV)
^{103}Rh (n, n') ^{103m}Rh	100	57.4 m	40	E_γ
^{109}Ag (n, n') ^{109m}Ag	48.65	39.2 s	87	E_γ
^{115}In (n, n') ^{115m}In	95.77	4.5 h	335	E_γ
^{137}Ba (n, n') ^{137m}Ba	11.32	2.6 m	661	660 ($E_{all} \simeq 1.9$ MeV)
^{197}Au (n, n') ^{197m}Au	100	7.4 s	407, 277 + 130	407
^{199}Hg (n, n') ^{199m}Hg	16.84	44 m	368 + 159	527
^{207}Pb (n, n') ^{207m}Pb	22.6	0.8 s	1060 + 565	1633

Remark: Nuclei can also be excited by other means, e.g. by photoactivation. Example: $^{103}Rh(\gamma, \gamma')^{103m}Rh$.

Some (n, n') reactions produce new radionuclides which are not observed in (n, p), (n, α) or (n, 2n) reactions. In consequence they are "characteristic" for the element concerned, and this can be of interest for analytical applications (18). Data are given in Table 3.7. The first one has been already practically examined by Anders (29).

TABLE 3.7
Production of "characteristic" isomers with measurable half-life by inelastic neutron scattering

Reaction	θ %	$T_{1/2}$	E_γ (keV)	E_x (keV)
$^{79}Br(n, n')^{79m}Br$	50.52	4.8 s	...	...
$^{89}Y(n, n')^{89m}Y$	100	14 s	913	913
$^{193}Ir(n, n')^{193m}Ir$	61.5	11.9 d	80	80
$^{204}Pb(n, n')^{204m}Pb$	1.48	68 m	912, 374, 899 (others)	2186

(5) *Response functions of threshold reactions in a fission neutron spectrum.* Apart from $\bar{\sigma}$, defined by equation (3.42), $\sigma(E)$ is also of great importance and it is even more fundamental. If the $\sigma(E)$ curve is well known for a given reaction, average and effective cross sections can be derived, and the effective threshold can be calculated (*cf.* Figure 3.1).

Experimental and calculated cross section curves or excitation functions for some important threshold reactions are represented in Figures 3.16 and 3.17. Actually, $\sigma(E)/\sigma_{eff}$ is plotted (reduced cross section curve). A compilation of some important cross section curves is given by Liskien and Paulsen (49). The function $\sigma(E)f(E)$ is called the response function. At higher neutron energy $f(E)$ becomes rather small in a reactor, hence $\sigma(E)f(E)$ will also decrease and practically one observes a "shifting" of the response curve towards lower neutron energy as compared to the corresponding cross section curve. This can be seen from Figures 3.18 and 3.19, where the response functions of various threshold reactions are represented.

Graphical integration of the response function allows the determination of $\bar{\sigma}$ (*cf.* Figure 3.20).

(6) *Calculation of a reaction rate in a fission neutron spectrum.* The reaction rate per atom is given by

D

$$R = \int_0^\infty \sigma(E) f(E)\,dE = \bar{\sigma} \int_0^\infty f(E)\,dE = \bar{\sigma} \cdot \bar{\varphi} \qquad (3.46)$$

where $\bar{\sigma}$ = the average cross section in a fission neutron spectrum

$\bar{\varphi}$ = the "equivalent fission flux"

$= \int_0^\infty f(E)\,dE$. The determination of $\bar{\varphi}$ is described in section VI, B, 3 of this chapter.

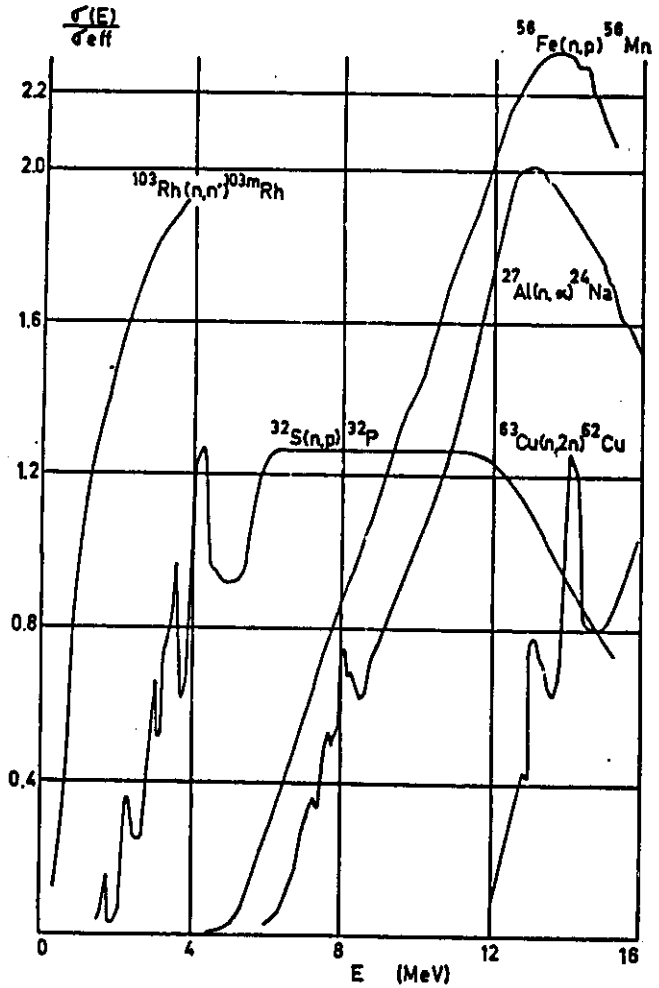

Fig. 3.16. Reduced cross section curves for some threshold reactions.

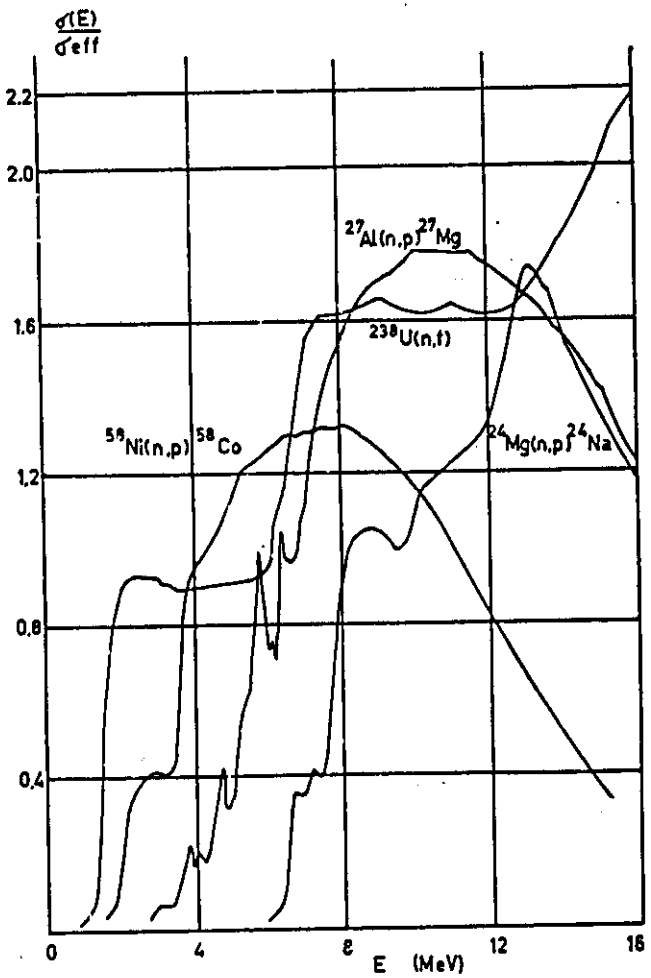

Fig. 3.17. Reduced cross section curves for some threshold reactions.

This can be of practical interest to calculate interferences in activation analysis (see Chapter 10, section II, C), such as:

Determination of	Interfering reaction
Fe in Co	$^{59}Co(n, p)^{59}Fe$
P in S	$^{32}S(n, p)^{32}P$
Cu in Zn	$^{64, 67}Zn(n, p)^{64, 67}Cu$
Na in Al	$^{27}Al(n, \alpha)^{24}Na$
Mn in Fe	$^{54, 56}Fe(n, p)^{54, 56}Mn$
Co in Ni	$^{58, 60}Ni(n, p)^{58, 60}Co$
Sc in Ti	$^{46, 47, 48}Ti(n, p)^{46, 47, 46}Sc$

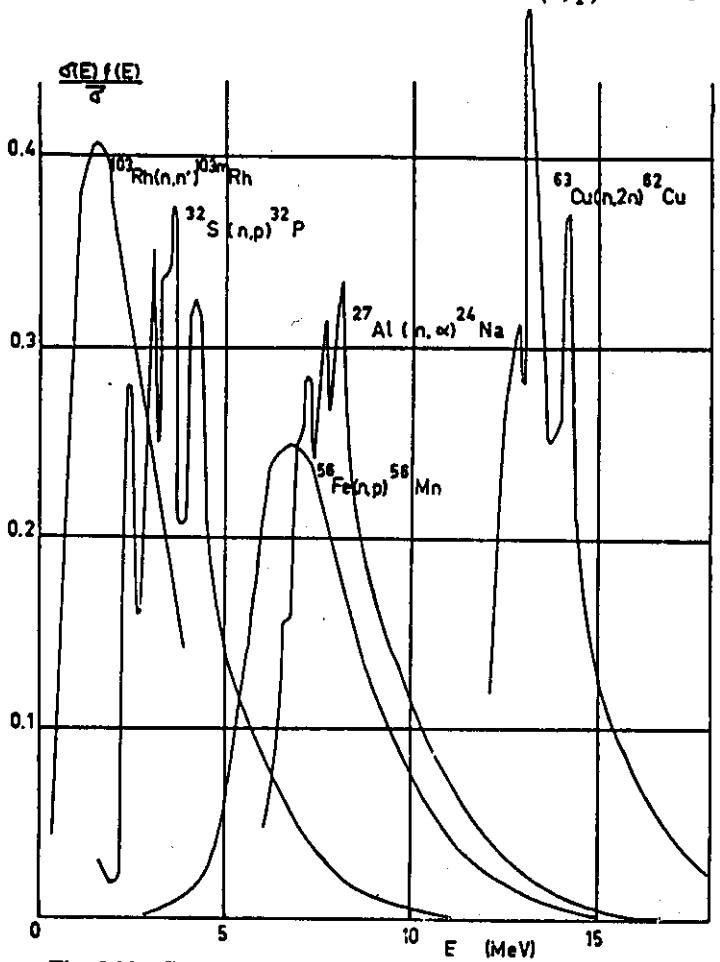

Fig. 3.18. Response functions for some threshold reactions.

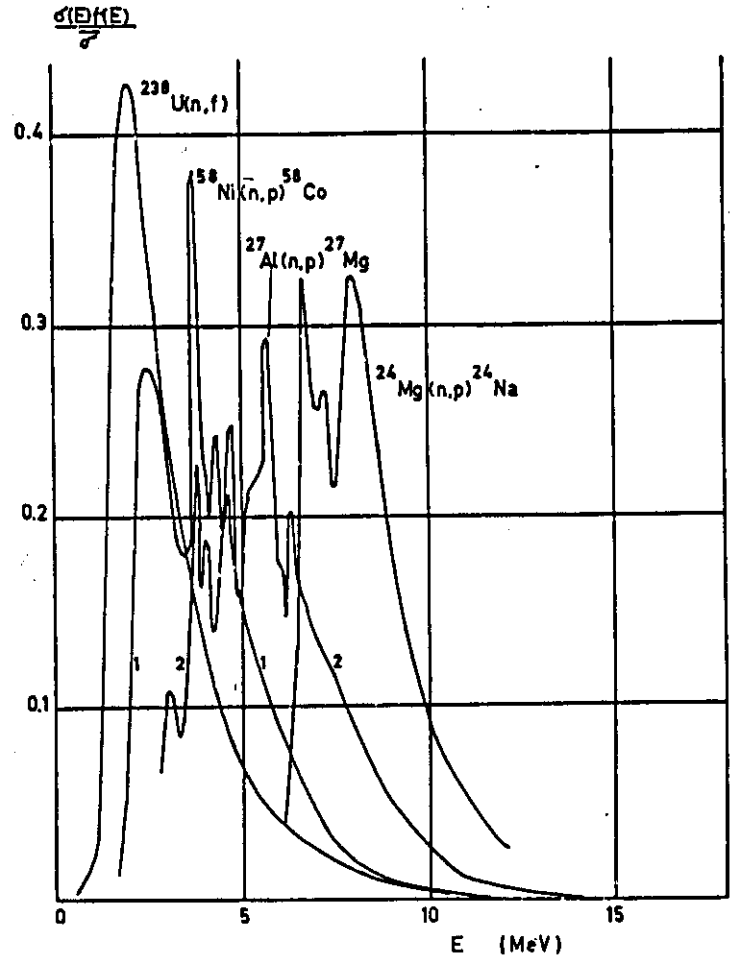

Fig. 3.19. Response functions for some threshold reactions.

Example: $^{56}Fe(n, p)^{56}Mn$; $\bar{\sigma} = 0.93$ mb $= 0.93 \times 10^{-27}$ cm^2

If $\varphi_{th} = 7.10^{13}$ n cm^{-2} s^{-1} and $k = 0.033$, $\bar{\varphi} = k\varphi_{th} = 2.3 \times 10^{12}$ n cm^{-2} s^{-1}. Hence $R = \bar{\sigma} \times \bar{\varphi} = 2.14 \times 10^{15}$ s^{-1}.

For practical use in activation analysis, reference is made to equation (10.1) which takes into account the weight of the irradiated element, the irradiation time and the half-life of the product radionuclide.

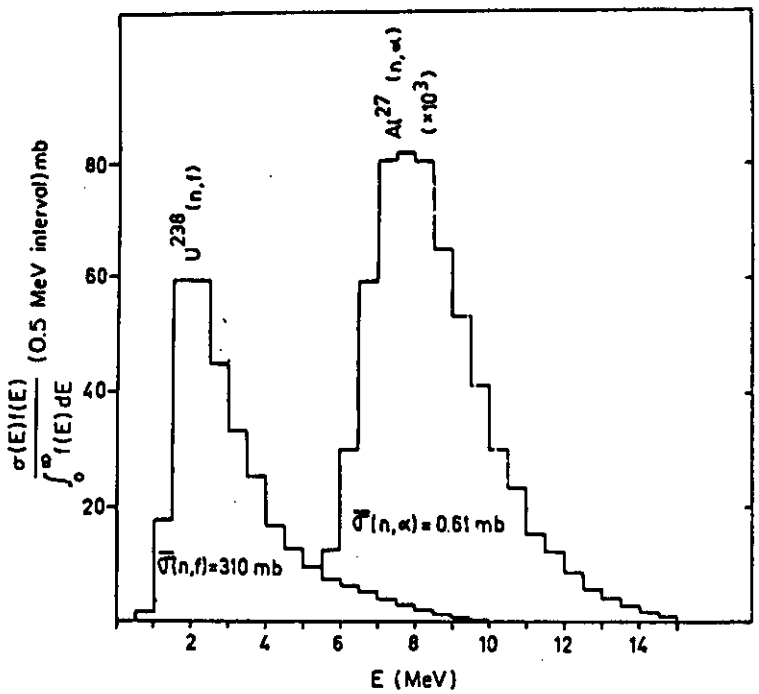

Fig. 3.20. Average fission neutron cross section per 0.5 MeV interval for $^{238}U(n, f)$ and $^{27}Al(n, \alpha)$. (51)

VI. Some Applications of Neutron-Induced Reactions

(A) The Cadmium Ratio (CR); Thermal/Resonance Flux Ratio

Cadmium has a very high absorption cross section for neutrons with an energy less than ~0.4–0.5 eV (Figure 3.4), due to the reaction $^{113}Cd(n, \gamma)^{114}Cd$. ^{114}Cd is not radioactive. The effective cadmium cut-off depends on the foil thickness and on the geometry (Table 3.4).

If a sample during the neutron irradiation is covered with a cadmium foil of 0.7–1 mm thickness, the thermal neutrons are screened out, so that (n, γ) reactions in the sample are only possible with "epicadmium" neutrons. Without cadmium cover, activation occurs as well with thermal as with resonance neutrons.

The measured ratio of the two activities for a given irradiation position is called the cadmium ratio (CR) of the nuclide of interest:

$$CR = \frac{\text{activity without Cd foil}}{\text{activity with Cd foil}} = \frac{\varphi_{th}\sigma_0 + \varphi_e I}{\varphi_e I} \tag{3.47}$$

Hence:

$$CR - 1 = \frac{\varphi_{th}\sigma_0}{\varphi_e I} \tag{3.48}$$

where φ_{th} = the conventional thermal neutron flux up to the Cd cut-off (E_{Cd}); $\varphi_{th} = n_{th}v_0 \approx nv_0$;

φ_e = epicadmium flux or resonance flux ($> E_{Cd}$)

(equations (3.17) and (2.26)).

It is obvious that the measured CR depends on the sensitivity of the detector for resonance and thermal neutrons, so that equation (3.48) does not directly give the real thermal to resonance flux ratio, unless this sensitivity is known (thermal activation cross section σ_0 and activation resonance integral $I = I' + I_{1/v} = I' + 0.45\ \sigma_0$ for 1 mm Cd-cover).

In the case of a $1/v$ detector, such as B, Na, Al, ... these calculations are quite simple ($I' = 0$). The induced activity under cadmium is, however, very small, so that very high cadmium ratios are found; even within a graphite lattice, where the φ_e/φ_{th} ratio can be as high as 1/13, one finds cadmium ratios of 33.

For that reason one prefers a detector with (a) prominent resonance peak(s); both with and without cadmium sufficient activity will then be induced. Widely used detectors are Co, Au and In. However, very thin foils must be irradiated to avoid thermal and/or resonance self-shielding (Chapter 10, section II, B, 4).

To illustrate the effect of neutron absorption on the determination of cadmium ratios, Høgdahl (14) mentions that the uncorrected cadmium ratio for gold in a pneumatic tube of a reactor is 12.5 using a 1 mil thick gold foil, while $CR = 5.5$ is found by using a dilute solution of gold (72 μg Au/ml). The difference is primarily due to self absorption of resonance neutrons. If gold foils are used, absorption corrections are necessary if the gold thickness exceeds about 0.5 mg/cm². It is, therefore, advisable to use dilute alloys, e.g. 1 w-% in aluminium, as neutron shielding then becomes negligible. Some experimental data for cobalt are given in Table 10.4.

If no self absorption occurs, the ratio resonance/thermal flux can be calculated from equation (3.48), after measuring the activities induced in the bare and cadmium covered detector.

Example: Co monitor, $\sigma_0 = 37.2$ barn, $I = 65$ barn ($+1/v$-contribution). If $CR_{Co} = 10.2$ is found, one calculates $\varphi_{th}/\varphi_e = (65/37.2) \times 9.2 = 16.1$.

The cadmium ratios for some irradiation positions in the BR–1 graphite reactor (Mol-Donk, Belgium), as determined with cobalt, are given in Table 3.8 (48).

TABLE 3.8
Cadmium ratios and fast to thermal flux ratios in BR–1 (48)

Position:	Thermal column	Rabbit X 26	Rabbit X 27	Rabbit X 28	Isotope Train	Channel	SBU	ITN
φ_{th}	2×10^{11}	4×10^{11}	8×10^{11}	1.4×10^{12}	4×10^{11}	8×10^{11}	—	—
$CR_{(Co)}$	—	63.6	10.2	10.85	13.41	7.42	10.4	7.94
$k=\bar{\varphi}/\varphi_{th}$†	1/200	1/261	1/12	1/16.7	1/18.4	1/5.92	—	—

† see equation (3.58).

The CR is often given or measured for gold. By using equation (3.49) one can find the CR for any nuclide expressed in terms of the CR for gold:

$$CR_X = 1 + (CR_{Au} - 1)\frac{I_{Au}\sigma_{0,x}}{\sigma_{0,Au} I_x} = 1 + (CR_{Au} - 1)\frac{1543\sigma_{0,x}}{98.8 I_x} \quad (3.49)$$

In the same way the CR for a nuclide can be expressed in terms of the CR for cobalt:

$$CR_X = 1 + (CR_{Co} - 1)\frac{65\sigma_{0,x}}{37.2 I_x} \quad (3.50)$$

Numerical data for σ_0 and I are given in Appendices 1 and 2.

Whatever detector is used, the CR is proportional to the thermal to resonance flux ratio. The greater the CR, the more the neutrons are thermalized.

Cadmium covers are also useful to screen out thermal neutrons in cases where thermal activation is undesirable, e.g. for the study of the fast neutron flux, see section VI, B, 3 of this chapter. The CR allows the calculation of the net thermal flux by correcting the induced activity for the resonance contribution, see section VI, B, 1 of this chapter. In some cases, fast neutrons are undesirable, e.g. owing to

interfering (n, p) or (n, α) reactions. By subtracting the activity, induced under cadmium, from the total activity, induced in the bare sample, one obtains the net thermal reaction rate. Interfering reactions can better be avoided by choosing an irradiation position with a high CR, such as the thermal column, although the sensitivity then decreases, as the total and thermal fluxes also decrease (Table 3.8).

The cadmium depresses the thermal flux density and gives also a perturbation in the intermediate neutron flux density. Sometimes it is even impossible to use a cadmium cover, e.g. because of temperature or safety conditions inside a reactor. In an alternative technique two detectors with different cross section curves can be used. For long irradiations, the detector couple Ag and Co seems most suitable:

^{59}Co: $\sigma_0 = 37.2$ b; $I = 65$ b

^{109}Ag: $\sigma_0 = 3.2$ b; $I = 47.5$ b (for production of ^{110m}Ag)

Absolute counting of ^{60}Co offers no special difficulties. The standardization of ^{110m}Ag can be accomplished with special counting techniques (sum-coincidence method; semiconductor counting, using the 656 keV photo peak; the efficiency of the semiconductor detector can be determined by means of a calibrated ^{137}Cs-source, $E_\gamma = 663$ keV). According to Høgdahl (14) one can write:

$$R_1 = \varphi_{th}\sigma_{0_1} + \varphi_e I_1 \text{ for detector 1}$$

$$R_2 = \varphi_{th}\sigma_{0_2} + \varphi_e I_2 \text{ for detector 2}$$

R_1 and R_2 are calculated from the absolute counting if the irradiation time and the decay time are known (e.g. equation (3.54)), hence one can determine $\varphi_{th} = [n_{th}v_0]_0^{0.5\,eV}$ and φ_e

$$\varphi_{th} = \frac{R_1 I_2 - R_2 I_1}{\sigma_{0_1} I_2 - \sigma_{0_2} I_1} \quad (3.51)$$

$$\varphi_e = \frac{R_2\sigma_{0_1} - R_1\sigma_{0_2}}{\sigma_{0_1} I_2 - \sigma_{0_2} I_1} \quad (3.52)$$

The assumption has been made that self-shielding corrections for thermal and resonance neutrons are negligible.

(B) Neutron Spectra (Particularly in Nuclear Reactors)

The response of an element in a given neutron spectrum depends on $\sigma(E)$ and on the neutron energy distribution. For a graphite moderated

reactor, the thermal neutrons have – in the ideal case – a Maxwell distribution, the resonance neutrons follow the dE/E-law, the fission neutrons the Watt distribution (see Chapter 4). To obtain a picture of the present stage of development in the detection, dosimetry and standardization of neutron radiation, the reader is referred to the IAEA Proceedings of the Symposium, held in Harwell, 10–14 December 1962 (31).

1. *Determination of the thermal flux*

Most elements have a σ, which follows the $1/v$-law at low neutron energy. The thermal flux is determined by absolute counting of the activity, which during a given irradiation time is induced in $1/v$ detectors, whose activation cross section is accurately known:

^{59}Co: $\sigma_0 = 37.2$ b; ^{60}Co: $\lambda = 4.168 \times 10^{-9}$ s^{-1}

^{197}Au: $\sigma_0 = 98.8$ b; ^{198}Au: $\lambda = 2.98 \times 10^{-6}$ s^{-1}

To avoid self-shielding (Chapter 10, II, B, 4) these elements are irradiated as dilute Al-alloys, e.g. 0.1–1 *w*-% Co or Au in Al. Due to resonance peaks in the $\sigma(E)$ curve, they are also activated by resonance neutrons. The reaction rate per atom of a "bare" detector, following the convention of Høgdahl (14), is given by equation (3.26);

$$R = R_{th} + R_e = \varphi_{th}\sigma_0 + \varphi_e I \qquad (3.53)$$

where R_{th} and R_e = thermal and epicadmium reaction rates;
φ_{th} ($=n_{th}v_0$) and φ_e = conventional thermal and epicadmium fluxes;
σ_0 = 2200 m/s activation cross section;
I = activation resonance integral, including $1/v$-tail.

The disintegration rate D (disintegrations per second) for an irradiation time t_b and a waiting time t is (Chapter 5, section III and equation 10.1).

$$D = N.R\,[1 - \exp(-\lambda t_b)] \exp(-\lambda t) \qquad (3.54)$$

or

$$D = N\varphi_{th}\sigma_{reactor}\,[1 - \exp(-\lambda t_b)] \exp(-\lambda t)$$

where N = number of target nuclei

$\sigma_{reactor}$ = given by equation (3.28).

If the detector is covered with cadmium, only resonance (epicadmium) activation occurs

$$R_e = \varphi_e I$$

Hence

$$D_e = N\varphi_e I\,[1 - \exp(-\lambda t_b)] \exp(-\lambda t) \qquad (3.55)$$

The net thermal activation is thus given by

$$D_{th} = D - D_e = N\varphi_{th}\sigma_0\,[1 - \exp(-\lambda t_b)] \exp(-\lambda t) \qquad (3.56)$$

Absolute counting of the induced activities D and D_e (without and with cadmium cover respectively) yields φ_{th}, as σ_0, N, λ, t_b and t are known. It is obvious that slightly different results will be found, depending on the thickness of the cadmium cover (different cadmium cut-off, see Table 3.2); the departure of the cross section from the $1/v$ law and the temperature dependence must also be considered in accurate neutron dosimetry. A practical determination can be found in Ref. 32. According to Hughes (2) the thermal flux at a particular point is known at best only to ±5%.

Much confusion is possible if one does not specify what convention is followed, e.g. whether the resonance integral includes the $1/v$-tail or not. In recent publications there is a preference for the Westcott formalism (9,10). Other conventions are those of Horowitz and Tretiakoff (33) and the unified formalism of Nisle (34). The simplest approach is that of Høgdahl (14), which was followed in the above discussion.

As will be explained in Chapter 10, the knowledge of the absolute thermal neutron flux is not required in activation analysis, as a comparator method is used in practice.

Absolute counting techniques are described in Chapter 4, section III, F.

2. *Determination of intermediate neutron spectra*

The conventional epicadmium flux φ_e can be determined by absolute counting of the activity, induced in a cadmium covered nuclide, whose resonance activation integral I is well known; (equation 3.55). Again, diluted alloys should be irradiated, to avoid resonance self absorption. When using or presenting resonance integral cross sections, it is necessary to state the lower energy limit (e.g. 0.5 eV, 0.55 eV, 5 kT, ...), the $1/v$ contribution and the correction factors used. The recommenda-

tions of the EANDC (European–American Nuclear Data Committee, see Ref. 15) should be followed.

Some values for resonance integral cross sections, as recommended by the Euratom Working Group on Dosimetry (37) are given in Table 3.9.

Actually there are no adequate methods for the experimental determination of φ as a function of E for neutrons of intermediate energy (up to ~1 MeV). For that reason, this energy region must be determined by theoretical predictions from the entire neutron spectrum, assuming a $1/E$ distribution in the epicadmium region. This analysis should then be coupled to experimental data from the few measurements that are possible at thermal and high (>1 MeV) energy.

Carver and Morgan (35) proposed to study the intermediate neutron spectrum by activating a series of thin wires (0.5 mm diameter), each of which possesses a distinct prominent capture resonance. Diluted Al-alloys (0.05–5 *w*-%) of Lu, Eu, Ir, In, Au, W, Se, As, La and Cd were used, giving resonances from 0.143 to 120 eV. Several methods of extracting this information are possible and the search for the optimum method is still in progress.

Other methods including resonance reactions, such as the sandwich-foil or the gold-difference technique, are reviewed by Moteff (36.) An extensive review is given by Zijp (12), who concludes that the whole field of intermediate neutron measurements is an underdeveloped region. Additional information can be found in Ref. 31.

It is not yet justified to make recommendations for a standard procedure, while for many resonance reactions the required resonance data are not sufficiently well known.

3. *Determination of the fast neutron spectrum in a reactor*

The neutron energy region above ~1 MeV is studied by means of threshold reactions, mostly (n, p), but also (n, α), (n, fission), (n, 2n) and even (n, n') reactions. The reaction rate for a threshold reaction is given by equation (3.46), $R = \bar{\varphi} \cdot \bar{\sigma}$, where $\bar{\varphi}$ is the equivalent fission flux, and $\bar{\sigma}$ the average cross section in a fission neutron spectrum. The absolute activity D_f (in disintegrations per second) for an irradiation time t_b and a waiting time t is thus

$$D_f = N\bar{\sigma}\bar{\varphi}[1 - \exp(-\lambda t_b)]\exp(-\lambda t) \qquad (3.57)$$

TABLE 3.9

Values for resonance integral cross sections, as recommended by the Euratom Working Group on Dosimetry (37)

Nuclide	$T_{1/2}$ formed	Resonance energy (eV)	I' (barn)	$I(1/v)$ (barn)		$I = I' + I(1/v)$ (barn)		σ_0 (barn)
				a	b	a	b	
^{115}In	54.2 m	1.457	2000 ± 300	60	68	2060 ± 300	2068 ± 300	166 ± 2
^{197}Au	2.70 d	4.906	1505 ± 20 (a) 1507 ± 20 (b)	38 ± 0.2	44 ± 0.2	1543 ± 20	1551 ± 20	98.8 ± 0.3
^{59}Co	5.26 y	132	50 ± 12	15	17	65 ± 12	67 ± 12	37.2 ± 1.5
^{63}Cu	5.1 m	227	1.2 ± 0.5	0.9	1	2.1 ± 0.5	2.2 ± 0.5	1.8 ± 0.4
^{55}Mn	2.58 h	337	6.0 ± 1.2	5.1	5.8	11.1 ± 1.2	11.8 ± 1.2	13.3 ± 0.2
^{63}Cu	12.8 h	580	2.4 ± 0.5	1.7	2	4.1 ± 0.5	4.4 ± 0.5	4.51 ± 0.23

(a) Cadmium cut-off energy 0.68 eV for a flat cylindrical cadmium cover with thickness of 1 mm in an isotropic flux density of neutrons.

(b) Cadmium cut-off energy 0.52 eV for a 1 mm cadmium cover in collimated beam of neutrons.

where N = number of target nuclei, and λ = disintegration constant for the radionuclide formed. Absolute counting of D_f yields $\bar{\varphi}$, if $\bar{\sigma}$ is known. Some frequently used threshold reactions are presented in Table 3.10. It is always desirable to irradiate several threshold detectors with different E_{eff} values, e.g. ^{58}Ni (n, p)^{58}Co (2.6–5 MeV), ^{27}Al(n, p), ^{27}Mg (4.3–5.3 MeV), ^{24}Mg (n, p)^{24}Na (6.3 MeV), ^{27}Al(n, α)^{24}Na (7.3–8.8 MeV) . . . , each of them yielding a value of $\bar{\varphi}$. If always the same $\bar{\varphi}$ is found, this indicates that the reactor fast flux at the irradiation position concerned approximates well a pure fission spectrum above say 1–3 MeV. The most frequently used threshold reaction is ^{32}S(n, p)^{32}P, $\bar{\sigma}$ = 65 mb. Irradiations for threshold reactions are mostly carried out under cadmium (0.7–1 mm) to limit thermal activation of the matrix and of some impurities, which would produce the same radionuclide; example: Na-impurity gives ^{24}Na by (n, γ) reaction, thus interfering with the reactions ^{27}Al(n, α)^{24}Na and ^{24}Mg(n, p)^{24}Na in Al or Mg respectively.

Some general requirements for a threshold detector are:

the material should contain only one or predominantly one stable isotope, to minimize the possibility for competing reactions;

the material should be available with as high a purity as possible;

the reaction should have a well known average cross section $\bar{\sigma}$ of convenient magnitude for fission neutrons with a good agreement between experimental and calculated values;

the product nuclide should have a well known – and preferably a simple – disintegration scheme, and a suitable half-life, and have possibilities for rather simple absolute activity determination;

the product nuclide should be the only remaining longer lived radioactive one produced by irradiation, so that counting should be possible without chemical separation.

If the reactor is "stable", i.e. the ratio fast/thermal flux is constant, irradiation of a threshold detector can be avoided and replaced by a thermal flux monitor. For that purpose, a factor k is introduced, which is defined as follows:

$$k = \frac{\bar{\varphi}}{\varphi_{reactor}} \approx \frac{\bar{\varphi}}{\varphi_{th}} \tag{3.58}$$

Indeed, the reaction rate is given by $R = \bar{\varphi} \times \bar{\sigma} = k \times \varphi_{th} \times \bar{\sigma}$. φ_{th} can be determined, as described in section VI, B, 1 of this chapter; $\bar{\sigma}$ being known for a threshold reaction, k can be calculated for this reaction and for the irradiation position used, if the induced activity is absolutely counted (D).

A simple method to determine $\bar{\varphi}/\varphi_{th}$ without absolute counting is to use $(NH_4)_2HPO_4$ and $(NH_4)_2SO_4$ as flux monitors. The thermal flux gives rise to the reaction ^{31}P(n, γ)^{32}P (σ_0 = 0.19 b), whereas the fast flux induces the threshold reaction ^{32}S(n, p)^{32}P ($\bar{\sigma}$ = 65 mb). As both reactions yield the same isotope, only a simple relative measurement is required to obtain $\bar{\varphi}/\varphi_{th}$:

$$\frac{\bar{\varphi}}{\varphi_{th}} = \frac{0.19 \times A_{n,p} \times N_p}{0.065 \times A_{n,\gamma} \times N_s} \tag{3.59}$$

where N_s and N_p are the number of target atoms resp. of ^{32}S and of ^{31}P; $A_{n,p}$ and $A_{n,\gamma}$ are the ^{32}P activities isolated from $(NH_4)_2SO_4$ and $(NH_4)_2HPO_4$ respectively.

If for several threshold reactions with widely varying E_{eff} values the same k-factor is found for a given irradiation position, this means that the fast reactor flux can be considered as an unperturbed fission flux. For the NRX and NRU reactors at Chalk River, the k-factor varies between 1/30 and 1/200 (25). Data for the BR–1 graphite-moderated reactor at Mol-Donk (Belgium) are given in Table 3.8.

A third method starts from the standard reaction ^{238}U(n, f), with a low effective threshold energy (E_{eff} = 1.5 MeV), $\bar{\sigma}$ = 310 mb. After chemical separation and absolute counting of a single fission product (e.g. ^{139}Ba, fission yield 5.1%), $\bar{\varphi}$ can be calculated. Using this value of $\bar{\varphi}$, one can determine $\bar{\sigma}$ of another well known reaction with a high effective threshold, such as ^{27}Al(n, α)^{24}Na, $E_{eff} \simeq$ 8.5 MeV. If $\bar{\sigma}$ = 0.61 mb is found – the preferred literature value of several independent investigators – one can conclude that the fast flux has the characteristic fission distribution above 0.5 MeV.

The following method is an absolute one. If $\sigma(E)$ is known, and $f(E)$ is supposed to be the Watt distribution, $\sigma(E) \times f(E)$ can be calculated step by step and graphically integrated. For ^{238}U(n, f) one calculates in this way $\bar{\sigma}$ = 310 mb and for ^{27}Al(n, α), $\bar{\sigma}$ = 0.61 mb. (Figure 3.20.) If for a given irradiation position, a fission flux $\bar{\varphi}$ is measured, using for instance ^{32}S(n, p)^{32}P, $\bar{\sigma}$ = 65 mb as the threshold detector, which yields the above values 310 mb and 0.61 mb, this also indicates a fission distribution.

(n, 2n) reactions normally occur at neutron energies, higher than those which are of real interest for reactor studies. The reaction

^{55}Mn(n, 2n)^{54}Mn ($\bar{\sigma} \approx 0.16$ mb, $E_{eff} = 10.3$ MeV) might become useful in the future as a flux detector for long irradiations, because of the ^{54}Mn properties.

(n, f) reactions upon ^{238}U and ^{237}Np have rather low effective thresholds (~1.5 and 0.7 MeV respectively).

Besides (n, p), (n, α) and (n, f) reactions, (n, n') reactions can also be used, on condition that isomers with measurable half-life are formed. So one can replace the reaction ^{238}U(n, f) by ^{103}Rh(n, n')^{103m}Rh (Figure 3.16 and Table 3.9) (38). Ingley (39) reports studies with the reaction ^{137}Ba(n, n')^{137m}Ba, $T_{1/2} = 2.6$ m, $\bar{\sigma} = 0.22$ b, $E_\gamma = 660$ keV, $E_T \approx 0.66$ MeV, $E_{eff} \approx 1.9$ MeV.

In some cases it is possible to obtain information about more than one energy region by using an isotope, which gives different reaction products:

Example 1:

^{204}Pb(n, n')^{204m}Pb; $T_{1/2} = 67$ m; $\bar{\sigma} = 22$ mb; $E_{eff} = 2.3$–5 MeV

^{204}Pb(n, 2n)^{203}Pb; $T_{1/2} = 52$ h; $\bar{\sigma} = 3.3$–5 mb; $E_{eff} > 8.9$ MeV

Example 2:

^{58}Ni(n, p)^{58}Co; $T_{1/2} = 71.3$ d; $\bar{\sigma} = 102$ mb; $E_{eff} = 2.6$–5 MeV

^{58}Ni(n, 2n)^{57}Ni; $T_{1/2} = 37$ h; $\bar{\sigma} = 0.004$ mb; $E_{eff} = 12$–13.7 MeV

Example 3:

Fabry (40) has pointed out that when bare and cadmium covered indium foils are irradiated simultaneously, values for thermal, intermediate and fast flux densities can be obtained:

^{115}In(n, γ)^{116m}In; $T_{1/2} = 54$ m; $\sigma_0 = 155$ b; $I = 3595$ b yielding thermal and intermediate flux densities.

^{115}In(n, n')^{115m}In; $T_{1/2} = 4.53$ h; $\bar{\sigma} = 166$ mb; $E_{eff} \approx 1.5$ MeV yielding the fast flux density.

A compilation of methods and data is given by Zijp (11). The most commonly used reactions are summarized in Table 3.10. A number of publications concerning fast neutron dosimetry can be found in Ref. 31.

4. 14 MeV *neutron flux of neutron generators* ("*The Texas Convention*")

Copper is used as a flux monitor. Irradiation with 14 MeV neutrons

leads to the formation of ^{62}Cu ($T_{1/2} = 10$ min; β^+ emitter) by the reaction ^{63}Cu(n, 2n); $\sigma_{14\ MeV} \approx 500$ mb (Figure 3.6).

At the International Conference on Modern Trends in Activation Analysis, held at College Station, Texas, in April 1965, normalized conditions for the flux monitoring of a neutron generator were presented. A copper disk of 99.9% purity, either 1 or 2.5 cm diameter by 0.25 mm thickness, is irradiated for 1 m and measured after a 1 m decay by a 7.5 cm × 7.5 cm NaI(Tl) detector at 3 cm from the top surface of the crystal. (The thickness of the detector can may vary from 2 to 4 mm.)

The copper disk is mounted between two disks of polystyrene or lucite (0.05 cm thick by 3 or 4.5 cm diameter, depending on which size of copper disk is to be used) to ensure that all positrons emitted in the decay are annihilated in the immediate vicinity of the disk source. The resulting sandwich provides about 1 g/cm^2 of plastic on all sides of the copper disk.

Measurements are made on a multichannel analyzer incorporating an automatic life-time correction circuit. The midpoint of the real counting interval is used to correct for the decay. The absolute disintegration rate is determined by the method of Heath (41), *cf.* equation (6.48).

$$D = \frac{A_p}{PzAB} \tag{3.60}$$

where D = disintegration rate of the source;
A_p = 0.511 MeV photo peak area in counts/m (minus the contribution of the Bremsstrahlung from 2.9 MeV β^+);
z = calculated efficiency of the detector for the source geometry being used;
A = absorption correction for the plastic absorber and detector can;
B = branching ratio for the 0.511 MeV annihilation radiation;
P = experimental photo peak efficiency.

Heath (e.g. Ref. 42) has calculated the quantity $1/PzAB = 8.591$ for a 1 cm diameter disk and 8.703 for a 2.5 cm diameter disk. Multiplying the photo peak area A_p by this factor, one obtains directly the disintegration rate D with an accuracy of ±5%. This value is used as a measure for the neutron flux at the irradiation site (Texas Convention).

The obtained value, calculated for a decay time equal to zero, is divided by the area of the disk, giving the absolute activity per cm^2

TABLE 3.10

Data for threshold reactions

Reaction	Absolute counting	Remark
^{27}Al (n, α) ^{24}Na $T_{1/2}$ = 15.0 h $\bar{\sigma}$ = 0.61 mb E_T = 3.26 MeV E_{eff} = 8.8 MeV (25)	$E_{(\gamma_1)}$ = 1.368 MeV (100%) $E_{(\gamma_2)}$ = 2.754 MeV (100%): γ–γ coincidence	Al should be free of Na and irradiated under Cd to reduce ^{24}Na activity from ^{23}Na (n, γ) reaction.
^{32}S(n, p) ^{32}P $T_{1/2}$ = 14.3 d $\bar{\sigma}$ = 65 mb E_T = 0.96 MeV E_{eff} = 3.9 MeV (25)	pure β–emitter $E(\beta)$ = 1.7 MeV (100%): Calibrated GM tube; 4π-proportional counter; liquid scintillation counting	Contribution of reaction ^{31}P (n, γ) ^{32}P from P–impurity should be checked by irradiation with and without Cd cover. Chemical form: $(NH_4)_2SO_4$. Chemical separation of ^{32}P activity. For irradiation in high neutron fluxes it is better to use sulphur pills.
^{54}Fe (n, p) ^{54}Mn $T_{1/2}$ = 303 d $\bar{\sigma}$ = 66 mb E_T = −0.16 MeV E_{eff} = 4.3 MeV (25)	$E(\gamma)$ = 0.835 MeV (100%): γ–spectrometry	Let ^{54}Mn from ^{54}Fe (n, p) decay ($T_{1/2}$ = 2.6 h). Eliminate ^{59}Fe activity from ^{58}Fe (n, γ) and possible ^{60}Co activity from Co-impurity by chemical separation Mn/Fe + Co or by γ–spectrometry (^{59}Fe 1.13–1.31 MeV; ^{60}Co: 1.17–1.33 MeV). Or use iron depleted in ^{58}Fe and enriched in ^{54}Fe
^{58}Ni (n, p) ^{58} (m)Co $T_{1/2}$ = 9.13 h (m) 71.3 d $\bar{\sigma}$ = 28 mb (m) 74 mb E_T = −0.62 MeV E_{eff} = 4.1 MeV (25)	$E_{(\gamma)}$ = 0.810 MeV (99%): γ–spectrometry, preferably with Ge(Li) detector of known efficiency (to avoid spectral interference from 0.863 MeV photopeak). Special coincidence technique possible (49): β^+ particles detected with coincidence selector using two scintillation probes for 0.511 MeV annihilation. The 810 keV γ–quanta are detected with third γ–detector. Coincidences between signals of third detector and coincidence signals from the other two detectors are measured	No chemical separation necessary. Ni should be free of Co to avoid ^{60}Co activity from the reaction ^{59}Co (n, γ). Attention: burn-up of $^{58(m)}$Co: σ_0 = 1650 b; σ_0(m) = 170,000 b
^{103}Rh (n, n') ^{103m}Rh $T_{1/2}$ = 58.7 m $\bar{\sigma}$ = 400 mb (52) E_{eff} = 0.6 MeV	I.T.: 40 keV, large internal conversion gives 20 keV X-ray; special counting technique (Ref. 38)	Interesting because of low E_{eff}. But: Ir-impurity (^{193}Ir, even for Cd-covered detector)
^{235}U (n, f) $\bar{\sigma}$ = 310 mb E_{eff} = 1.5 MeV	^{140}La (daughter of ^{140}Ba, fission yield 5.7%) $E_{(\gamma)}$ = 1.6 MeV ^{137}Cs (fission yield 6.1%): $E_{(\gamma)}$ = 0.663 MeV, well-known decay scheme: γ-spectrometry	Uranium depleted in ^{235}U (about 10 ppm ^{235}U)

and per min (D'). The flux F is then calculated from equation (3.61).

$$F = \frac{D'}{60\sigma N\theta[1 - \exp(-0.693t_b/T_{1/2})]} \qquad (3.61)$$

where σ = 14 MeV cross section for the reaction $^{63}Cu(n, 2n)^{62}Cu$ = 500 mb;
N = number of atoms/cm^2 = $6.02 \times 10^{23} \times w/63.5$, w being the weight of copper in g/cm^2 in the disk;
θ = isotopic abundance of ^{63}Cu = 0.69;
t_b = irradiation time = 1 m;
$T_{1/2}$ = half-life of ^{62}Cu = 10 m.

An activity of 10^7 d/m/g Cu (small copper disk) corresponds to an absolute neutron flux of 7.7×10^6 n cm^{-2} s^{-1}.

More practical for routine analysis is flux monitoring with a low geometry neutron counter (BF_3) to measure the neutron output during the irradiation. The measurement of ^{16}N formed by the $^{16}O(n, p)^{16}N$ reaction on the target cooling water has also been proposed (43). Several authors use a plastic scintillator (44, 45) although this counter is not specific for neutrons, so that other radiation is also detected, e.g. prompt gammas. Iddings (46) investigated the flux monitoring systems used with 14 MeV neutron generators, with special regard to oxygen analysis. The reference sample system was found to be the most accurate. In some cases an internal standard can be used (Chapter 10, section II, B, 4c(4)).

The $^{31}P(n, p)^{31}Si$ reaction (threshold: 1.9 MeV; cross section in the pertinent energy range $\approx$68 mb; product radionuclide $T_{1/2}$ = 2.6 h, $E(\beta)$ = 1.4 MeV, $E(\gamma)$ = 1.26 MeV) has been proposed for measuring the neutron yield from the D (d, n)^{3}He reaction (neutron energy about 2.6 MeV) (47).

(C) Determination of Activation Cross Sections

1. *Thermal activation cross section (σ_0) and activation resonance integral (I)*

As stated in section VI, A and B, the thermal and resonance fluxes for a given irradiation position in the reactor can be determined by irradiation of a cobalt or gold monitor with and without cadmium cover. In section V, C, 2, the EANDC recommendations were given to choose the thickness of the cadmium cover.

The thermal activation cross section of any nuclide X can directly be determined by absolute counting of the induced activity after elimination of the resonance activation ($R_{th} = R - R_e$). If the cross section follows the $1/v$ law, the thermal activation cross section σ_0(2200 m/s value) is obtained directly, by application of equation (3.62) as λ, t_b and t are known, whereas φ_{th} is determined by means of the gold or cobalt flux monitor. The disintegration rate must obviously be calculated for a decay time equal to zero.

$$D_{th} = \varphi_{th}\sigma_0 N[1 - \exp(-\lambda t_b)] \cdot \exp(-\lambda t) \qquad (3.62)$$

Absolute counting (Chapter 4, section III, F) of the activated material is usually carried out with a calibrated Geiger-Müller counter (known efficiency), with a 4π-proportional counter (all betas are detected from the sample inside the counter) or by liquid scintillation counting. The absolute disintegration rate can also be calculated from the net photo peak area, using a NaI(Tl) or Ge(Li) detector, of which the efficiency is known as a function of geometry and γ-energy.

From the cadmium ratio CR_X, the total activation resonance integral I_X (including the $1/v$ tail) can be calculated as appears from equation (3.49) or (3.50). Indeed, CR_{Au} or CR_{Co} and CR_X are determined, $\sigma_{0,x}$ is found by absolute counting, whereas $\sigma_{0,Au}$ and I_{Au} (or $\sigma_{0,Co}$ and I_{Co}) are well known. The $1/v$ contribution of the total activation resonance integral can be calculated, as described in section V, C, 2 of this chapter.

Although the principle of activation measurements is quite simple, it is exceedingly difficult to obtain reproducible, accurate data in practice, with the result that many thermal activation cross sections are known to only about 20% (Ref. 2). The sources of error are described in Chapter 10. The efficiency of the counter for complex disintegrations, in which several β-energies, γ-rays, conversion electrons, or X-rays following electron capture may occur is sometimes hard to estimate. Moreover, the disintegration scheme and/or the exact half-life of some radionuclides is not sufficiently well known. As already stated in section VI, B, 1, one must specify what convention is followed (Westcott; Horowitz; Nisle; Høgdahl, . . .)

In some very special cases, $\sigma_{reactor}$ can be determined without absolute counting of the activation product of interest – thus without knowledge of the decay scheme – using a second-order reaction (Chapter 10, section II, C, 3). This has, for instance, been done for the

reaction $^{74}Ge(n, \gamma)^{75}Ge$ using the second-order reaction $^{74}Ge(n, \gamma)\ ^{75}Ge \xrightarrow{\beta^-} {}^{75}As(n, \gamma)^{76}As$ and for the reaction $^{190}Os(n, \gamma)^{191}Os$, using the second-order reaction $^{190}Os(n, \gamma)^{191}Os \xrightarrow{\beta^-} {}^{191}Ir(n, \gamma)^{192}Ir$ after determining the apparent arsenic and iridium concentrations in high-purity germanium and osmium respectively. Other possible reactions can be found in Table 10.8. If the cadmium ratios of Ge, Os, ... and of a cobalt or gold monitor are determined, σ_0/I can be computed using equation (3.49) or (3.50). From the experimentally determined value of $\sigma_{reactor}$ then follows σ_0 and I, using equation (3.28). In order to determine the thermal neutron flux, which is required for finding $\sigma_{reactor}$ (see Chapter 10, section II, C.3), an absolute counting of ^{60}Co or ^{198}Au is obviously required, but their disintegration scheme is well known.

2. *Average cross section in a fission neutron spectrum*

The reaction rate for a threshold reaction is given by equation (3.46). Absolute counting of the induced activity, yields $\bar{\sigma}$, if the equivalent fission flux $\bar{\varphi}$ is known (see section VI, B, 3 of this chapter). If the k-value (equation 3.58) for a given irradiation position is known (determined by means of a suitable standard such as $^{32}S(n, p)$) and k is constant as a function of time, monitoring of the thermal flux is, in principle, sufficient for the determination of the $\bar{\sigma}$ of a threshold reaction. As already stated above, irradiation is normally carried out under cadmium.

Determination of $\bar{\sigma}$ is possible without absolute counting, if the reaction product of the threshold reaction, e.g. $^{72}Ge(n, p)^{72}Ga$, can also be obtained by thermal activation, e.g. $^{71}Ga(n, \gamma)^{72}Ga$. ($\sigma_0 = 5.0 \pm 0.5$ b). (Obviously, a similar reaction scheme occurs when dealing with (n, α) reactions.) (26). In order to evaluate the contribution of each reaction, i.e. the formation of ^{72}Ga from the Ge-matrix and from the Ga-impurity, Ge and Ga samples are irradiated with and without cadmium cover. The obtained activities are given by:

$$A = a + b \tag{3.63}$$

$$A_{Cd} = a_{Cd} + b = \frac{a}{CR} + b \tag{3.64}$$

as

$$CR = a/a_{Cd} \tag{3.65}$$

Here: A_{Cd} and A = total ^{72}Ga-activities isolated from the Ge-samples after irradiation with and without cadmium cover;
a_{Cd} and a = ^{72}Ga-activities from the Ga-impurity in the Ge-samples with and without cadmium cover;
b = ^{72}Ga-activity due to the threshold reaction $^{72}Ge(n, p)^{72}Ga$ only;
CR = cadmium ratio of ^{71}Ga, determined by means of a Ga-standard.

Dividing equations (3.63) and (3.64) by the ^{72}Ga-activity of the Ga-standard, which is irradiated under the same conditions without Cd, yields the total "measured concentrations" C and C_{Cd} of the element Ga in both samples: (only simple, relative measurements)

$$C = C(n, \gamma) + C(n, p) \tag{3.66}$$

$$C_{Cd} = \frac{C(n, \gamma)}{CR} + C(n, p) \tag{3.67}$$

where $C(n, \gamma)$ is the "true concentration" of Ga in Ge;
$C(n, p)$ is the "apparent Ga concentration" in Ge, due to the (n, p) reaction with the matrix (*cf.* Chapter 10, section II, C, 1).
These two concentrations can be calculated from the measured activities, using equation (3.64) and (3.65).

$$C(n, \gamma) = (C - C_{Cd}) \frac{CR}{CR - 1} \tag{3.68}$$

$$C(n, p) = C - C(n, \gamma) \tag{3.69}$$

If the apparent Ge-concentration from the (n, p) reaction $C(n, p)$ is substituted into equation (10.34), $\bar{\sigma}(n, p)$ can be calculated, if $\bar{\varphi}/\varphi_{th}$ for the irradiation position is known (see section VI, B, 3 of this chapter).

References

1. Friedlander, G., and Kennedy, J. W., *Nuclear and Radiochemistry*, J. Wiley & Sons, New York, 1960.
2. Hughes, D. J., *Pile Neutron Research*, Addison-Wesley, Cambridge, Mass., 1953.
3. Grundl, J. A., and Usner, A., *Nucl. Sci. Eng.*, 8, 598 (1960).
4. Jung, R. C., Epstein, H. M., and Chastain, J., "A simple Experimental Method for Determining Effective Threshold Energies and Cross Sections", BMI-1486 (Dec. 1960).

5. Green, A. E. S., *Nuclear Physics*, McGraw-Hill, New York, p. 214, 1955.
6. Prud'homme, J. T., *Neutron Generators*, Texas Nuclear Corp., Austin, Texas, p. 6, 1962.
7. Levin, J. S., and Hughes, D. J., *Phys. Rev.*, 101, 1328 (1956).
8. Stoughton, R. W., and Halperin, J., *Nucl. Sci. Eng.*, 6, 100 (1959).
9. Westcott, C. H., Walker, W. H., and Alexander, T. K., *Proc. Int. Conf. on Peaceful Uses of Atomic Energy, Geneva*, 16, 70 (1958).
10. Westcott, C. H., "Effective Cross Section Values for Well-Moderated Thermal Reactor Spectra", *AECL-1101*, 1960.
11. Zijp, W. L., "Review of Activation Methods for the Determination of Fast Neutron Spectra", *RCN-37, Petten* (May 1965).
12. Zijp, W. L., "Review of Activation Methods for the Determination of Intermediate Neutron Spectra", *RCN-40, Petten* (October 1965).
13. Hughes, D. J., and Schwartz, R. B., "Neutron Cross Sections", *U.S. At. Energy Comm., Rept. BNL-325, 2nd ed.* 1958.
13b. Hughes, D. J., *Neutron Cross Sections* (Intern. Series Monographs on Nuclear Energy, Div. II (Vol. I), Pergamon, London 1957.
14. Høgdahl, O. T., "Neutron Absorption in Pile Neutron Activation Analysis", MMPP-226-1 (Dec. 1962).
15. Goldstein, H., Harvey, J. A., Story, J. S., and Westcott, C. H., "Recommended Definitions for Resonance Integral Cross Sections", *EANDC-12* (Oct. 1962).
16. Dresner, L., *Nucl. Energy*, 2, 118 (1955).
17. Flerov, N. N., and Talyzin, V. M., *J. Nucl. Energy*, 4, 529 (1957).
18. Schulze, W., "Fast Neutrons in Activation Analysis", *3e Congrès International de Biologie de Saclay* (Sept. 1963).
19. Neuert, H., and Pollehn, H., "Tables of Cross Sections of Nuclear Reactions with Neutrons in the 14–15 MeV Energy Range", *EUR 122e* (Brussels 1963).
20. Bormann, M., Cierjacks, S., Langkau, R., and Neuert, H., *Z. Phys.*, 166, 477 (1962).
21. Bayhurst, B. P., and Prestwood, R. J., *J. Inorg. Nucl. Chem.*, 23, 173 (1961).
22. Watt, B. E., *Phys. Rev.*, 87, 1037 (1952).
23. Cranberg, L., *et al.*, *Phys. Rev.*, 103, 662 (1956).
24. Leachmann, R. B., *Proc. Int. Conf. on Peaceful Uses of Atomic Energy, Geneva*, 2, 193 (1956).
25. Roy, J. C., and Hawton, J. J., "Tables of Estimated Cross Sections for (n, p), (n, α) and (n, 2n) Reactions in a Fission Neutron Spectrum", *CRC-1003* (Dec. 1960).
26. De Neve, R., Reaction Rates from Nuclear Reactor Neutrons. *Proc. of the "Koninkl. Vl. Academie voor Wetensch., Letteren en Schone Kunsten van België"*, XXX, 2, Brussels 1968.
27. Dzhelepov, B. S., and Peker, L. P., *Decay Schemes of Radioactive Nuclei*, Pergamon Press, Oxford, 1961.
28. Stelson, P., and Campbell, A., *Phys. Rev.*, 97, 1222 (1955).
29. Anders, O. U., *Anal. Chem.*, 34, 1678 (1962).
30. *CINDA*. An Index to the Literature on Microscopic Neutron Data, by USAEC Division of Technical Information Extension, USSR Nuclear Data Information Centre, ENEA Neutron Data Compilation Centre, IAEA Nuclear Data Unit, 1967, 1968, 1969 (and Supplements).

31. Neutron Dosimetry; *Proc. of the Symp. on Neutron Detection, Dosimetry and Standardization*, Harwell 10–14 Dec. 1962, IAEA, Vienna, 1963 (I and II).
32. Durham, R. W., and Girardi, F., *Nuovo Cimento*, 19, Supp. 1, Series X, 4 (1961).
33. Horowitz, J., and Tretiakoff, O. "Effective Cross Sections for Thermal Reactors", *EANDS(E) 14, Oak Ridge Meeting* (1960).
34. Nisle, R., *Proc. of the Symp. on Neutron Detection, Dosimetry and Standardization*, Harwell, 10–14 Dec. 1962, IAEA, Vienna, 1963, I, p. 111.
35. Carver, J. G., and Morgan, W. R., Modern Trends in Activation Analysis, *Proc. Internat. Conf. Texas* 1961, p. 19.
36. Moteff, J., *Nucleonics*, 20 (12), 56 (1962).
37. Beaugé, R., "Sections Efficaces pour les Détecteurs de Neutrons par Activation Recommandées par le Group de Dosimétrie d'Euratom" *Euratom* 1963.
38. Day, D. H., Fox, W. N., and Hyder, H. R., *AEEW-R 85* (1963).
39. Ingley, J. S., *TR-905* (1961).
40. Fabry, A., and Deworm, J. P., "Progress in the Use of Iron as a Neutron Flux Integrator", *Comm. Euratom Working Group on Dosimetry* (October 1964).
41. Heath, R. L., "Scintillation Spectrometry Gamma-ray Spectrum Catalogue" *Atomic Energy Division*, Idaho Falls, August 1964, Res. and Development Report IDO-16. 880, (I and II).
42. Cuypers, M., and Cuypers, J., *Gamma-ray Spectra and Sensitivities for 14 MeV Neutron Activation Analysis*, Texas A. & M. University, College Station, Texas, April 1966.
43. Meinke, W. W., and Shideler, R. W., *Nucleonics*, 20(3), 60 (1962).
44. Fujii, I., *et al.*; *J. At. Energy Soc. Japan*, 5, 455 (1963); Anal. Chim. Acta, 34, 145 (1966).
45. Girardi, F., Pauly, J., and Sabbioni, E., "Dosage de l'Oxygène dans les Produits Organiques et les Métaux par Activation aux Neutrons de 14 MeV", *EUR-2290f, Euratom* Brussels 1965.
46. Iddings, F., *Anal. Chim. Acta*, 31, 207 (1964).
47. Jessen, P. L., and Pierce, K. S., *Trans. Am. Nucl. Soc.*, 10(1), 85 (1967).
48. Speecke, A., Private communication.
49. de Swiniarsky, R., and Czerny, J., "Mesure de l'activité absolu d'une Source de ^{58}Co par un dispositif à coincidence", *CEA-CENG-Int-Pi-171-145* (1963).
50. Liskien, H., and Paulsen, A., "Compilation of cross sections for some neutron induced threshold reactions", *EUR-119e, Euratom Brussels*, 1963.
51. Durham, R. W., Navalkar, M. P., and Ricci, E., "Modern Trends in Activation Analysis", *Proc. Internat. Conf. Texas*, 1961, p. 67.
52. Köhler, W., and Knopf, K., *Nukleonik*, 10, 181 (1967).